12-1999

Role of fiber morphology in thermal bonding

Subhash Chand

Recommended Citation

To the Graduate Council:

I am submitting herewith a thesis written by Subhash Chand entitled "Role of fiber morphology in thermal bonding." I have examined the final electronic copy of this thesis for form and content and recommend that it be accepted in partial fulfillment of the requirements for the degree of Master of Science, with a major in Textiles, Retail, and Consumer Sciences.

<div align="right">Gajanan S. Bhat, Major Professor</div>

We have read this thesis and recommend its acceptance:

Joseph E. Spruiell, Kermit E. Duckett

<div align="right">Accepted for the Council:</div>
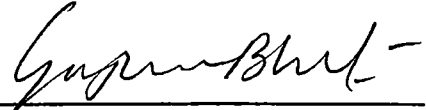
<div align="right">Carolyn R. Hodges</div>

<div align="right">Vice Provost and Dean of the Graduate School</div>

(Original signatures are on file with official student records.)

To the Graduate Council:

I am submitting herewith a thesis written by SUBHASH CHAND entitled "ROLE OF FIBER MORPHOLOGY IN THERMAL BONDING." I have examined the final copy of this thesis for form and content and recommend that it be accepted in partial fulfillment of the requirements for the degree of Master of Science, with a major in Textiles, Retailing & Consumer Sciences.

_____
Gajanan S. Bhat, Major Professor

I have read this thesis
and recommend its acceptance:

_____
Joseph E. Spruiell

_____
Kermit E. Duckett

Accepted for the Council:

_____
Associate Vice Chancellor
and Dean of the Graduate School

ROLE OF FIBER MORPHOLOGY IN THERMAL BONDING

A THESIS PRESENTED FOR THE

MASTER OF SCIENCE

DEGREE

THE UNIVERSITY OF TENNESSEE, KNOXVILLE

SUBHASH CHAND
DECEMBER 1999

DEDICATION

This thesis is dedicated to my father

Mr. Raghuvir Singh

and my sister-in-law

Mrs. Sunita

ACKNOWLEDGMENTS

ABSTRACT

The aim of this research was to investigate the thermal point bonding process. Primary objectives were to carefully understand the changes taking place in the fiber structure due to applied heat and pressure, and the role of fiber morphology in determining optimum process conditions and the properties of the webs. To study fibers with varying morphology, i.e., from partially drawn as in spunbonding to fully drawn as in staple fiber nonwovens, fibers with a wide range of crystallinity and orientation were spun and characterized from a polypropylene resin. Thermally bonded carded webs were produced using these fibers and characterized in order to understand thermal bonding behavior of fibers with different morphology. The fibers with different morphologies differed in their bonding behavior. The fibers with higher molecular orientation and crystallinity tended to form a weak and brittle bond due to lack of polymer flow and fibrillation of the fibers in the bonded regions. In general, fibers with lower molecular orientation and lower crystallinity yielded stronger and tougher webs. Fibers with relatively less developed morphology also exhibited lower optimum bonding temperature. Significant morphological changes in fibers were observed during the thermal bonding process, in bonded as well as unbonded regions of the web. As a final step to see how the observations from staple fiber study translate to one of the relevant process during scale-up, spunbond studies were also conducted.

TABLE OF CONTENTS

LIST OF TABLES

LIST OF FIGURES

LIST OF ABBREVIATIONS

1. PP = Polypropylene

2. SEM = Scanning Electron Microscope

3. MFR = Melt Flow Rate

4. WAXD = Wide Angle X-ray Diffraction

5. DSC = Differential Scanning Calorimetry

6. TMA = Thermo-mechanical Analysis

7. MD = Machine Direction

8. CD = Cross Direction

CHAPTER I

INTRODUCTION

The basic idea for thermal bonding was introduced by Reed [1] in 1942. Since then, there have been a number of developments in this field. Now, thermal bonding is the most popular method of bonding used in nonwovens. The main advantages of thermal bonding are low raw material and energy costs, products versatility, smaller space requirements, cleanliness of the process, better product quality characteristics, and increased production rates. Of the several types of thermal bonding such as area-bond calendering, point-bond calendering, through air bonding, ultrasonic bonding and radiant bonding, point bonding is the most widely used technique [2].

Nonwoven fabric properties are determined by the characteristics of bond points and in particular by the stress-strain relationship of the bridging fibers. During point bonding, the bond points and the bridging fibers develop distinct properties, different from those of the virgin fibers, depending on the process variables employed. This change in properties has been hinted at by several authors but has not been investigated. So far most of the work has been done to study the effects of bonding conditions on the fabric properties. Some work [3-5] has been done on the effect of fiber properties on final fabric properties. However, the role of fiber morphology in point bonding and morphological changes taking place in the fibers due to applied heat and pressure in thermal bonding have been almost untouched. This has been mainly due to the fact that it

1

is almost impossible to characterize the bond points and the fibers surrounding the bond without the use of some innovative techniques.

Because point bonding is used for a wide range of fibers, from those with less developed morphology as in spunbonding to those with fairly well developed morphology as in staple fibers, it is very important to investigate the effects of fiber morphology on bonding behavior of the fibers. The objectives of this research were:

1. To develop a good understanding of the effect of fiber morphology on bonding.

2. To examine what changes take place in the fibers in bonded region, unbonded region and bond vicinity during thermal bonding.

3. To be able to suggest optimum processing conditions for thermal bonding based on fiber morphology.

4. To understand how fiber properties translate into fabric properties.

Staple fibers with a wide range of crystallinity and orientation were produced and studied. As a final step to see how the observations using this study translate to one of the relevant processes during scale-up, spunbond trials were also conducted.

CHAPTER II

LITERATURE REVIEW

2.1 Introduction to Thermal Bonding

A formed web, both in pellet-to-product and fiber-to-product processes, lacks many of the characteristics of the desired nonwoven end product. The web is flexible, soft and porous but lacks strength and durability. To achieve a usable nonwoven product, the individual fibers must be, to some extent, connected. The connection process is called bonding.

The bonding method and materials employed determine, or at least influence, many properties of the end product. To meet the wide range of applications of nonwoven products, several bonding processes have been developed. Bonding methods can be characterized in several ways. By focussing on the method used to achieve the bond [6], a simple categorization is:

Mechanical

Chemical

Thermal.

Mechanical bonding basically involves fiber entanglement. This can be achieved through needle punching or fluid jet action. In many applications mechanical bonding is used as a first stage of bonding, followed by chemical or thermal bonding which impart additional strength and other desirable characteristics not attainable through needling alone.

3

Chemical bonding is a process of adding a nonfibrous material to a web during or after formation. There is a wide range of chemicals that can be used, and techniques for applying the chemicals. Post application heat treatment is necessary to dry, cure and/or fuse the binder. This process has been the workhorse of the nonwoven fabric market.

Thermal bonding process uses application of heat or heat and pressure to fuse the formed nonwoven web into a finished fabric [7]. Thermal bonding requires a thermoplastic component, which may be as a fiber, powder, film or hot melt or as a low-melt sheath on a bicomponent fiber. The bonding options available in thermal bonding are as follows [8]:

(a) **Area bond calendering**: This process produces materials that are stiff, thin, relatively inflexible, and strong. Products are film-like, but permeable.

(b) **Point bond calendering**: This process produces fabrics whose properties can range from thin, relatively inflexible, stiff and strong to bulky, elastic, soft and weak, depending on the size and density of bond points and other process conditions. Area and point bonding are normally used for nonwoven fabrics below 25-30 g/m^2 (medical and sanitary webs) and for medium basis weight nonwoven fabrics up to approximately 100 g/m^2 (interlining and filtration webs).

(c) **Through air bonding**: This produces materials that can be bulky, open, soft, strong, extensible, breathable, and absorbent. The method is predominantly used for medium and high basis weight nonwoven fabrics (geotextiles and carpet backing), as well as for nonwoven fabrics with high bulk for filtration and furniture applications.

4

(d) **Ultrasonic bonding**: This process works the material through rapid compressive deformations, thereby producing heat through internal friction of the polymer itself. This heating causes fibers to soften and bond. This process often uses a pattern or point bonding principle and can yield strong yet flexible and breathable products for specific applications.

(e) **Radiant heating**: Radiant heating is achieved by exposing the web to infrared radiation, which increases the temperature of the web and soften the binder component. Radiant bonding is often used for powder bonded nonwoven fabrics to produce materials that are flexible, soft, resilient, open and absorbent. It was also used to stabilize thin needle-punched fabrics by glazing one surface.

Thermal bonding is an important technology. It offers high production rates because bonding is accomplished at high productivity with heated calender rolls. It has been successfully used with a number of thermoplastic fibers. It offers significant energy conservation with respect to latex bonding because of effective thermal contact, and because no water needs to be evaporated after bonding. It is environmentally friendly because there are no residual ingredients to be disposed of. A wide range of fibers is available for thermal bonding. These include homofil and bicomponent fibers, which in turn allow a wide range of fabric properties and aesthetics to be obtained [2].

The most widely practiced thermal method is point bonding. Point bonding is applicable to carded, spun laid, and meltblown webs. PP fibers, by themselves or as binder fibers, are used most often for point bonding. Low melting copolymers of polyester are also used. Special sheath/core bicomponent fibers, where the core has a higher melting temperature, have also been developed for thermal bonding [2].

2.2 Point-Bonding Process Description

In a typical production line, the web is fed by an apron leading to a calender nip consisting of one engraved and one smooth roll. As the web enters the hot calender nip, the fiber temperature is raised to the point at which tackiness and melting cause fiber segments caught between the tips of engraved points and smooth roll to adhere together. The heating time is of the order of milliseconds. The process is schematically shown in Figure 2.1 [2].

The fabric emerging from the nip may be cooled by contacting two water-cooled rolls. Fiber shrinkage tendencies are accommodated by fabric relaxation; otherwise cooling takes place under tension, and a thin, 'boardy' fabric results. Fabric is then wound up under controlled tension into a roll of appropriate hardness and integrity [9]. Main process variables are bonding pressure, temperature and time.

2.3 Thermal Bonding: a Thermomechanical Process

Thermal bonding is a thermomechanical process and involves the following phenomena [2, 10]:

Heat transfer

Heat of deformation

Clapeyron effect

Flow

Diffusion
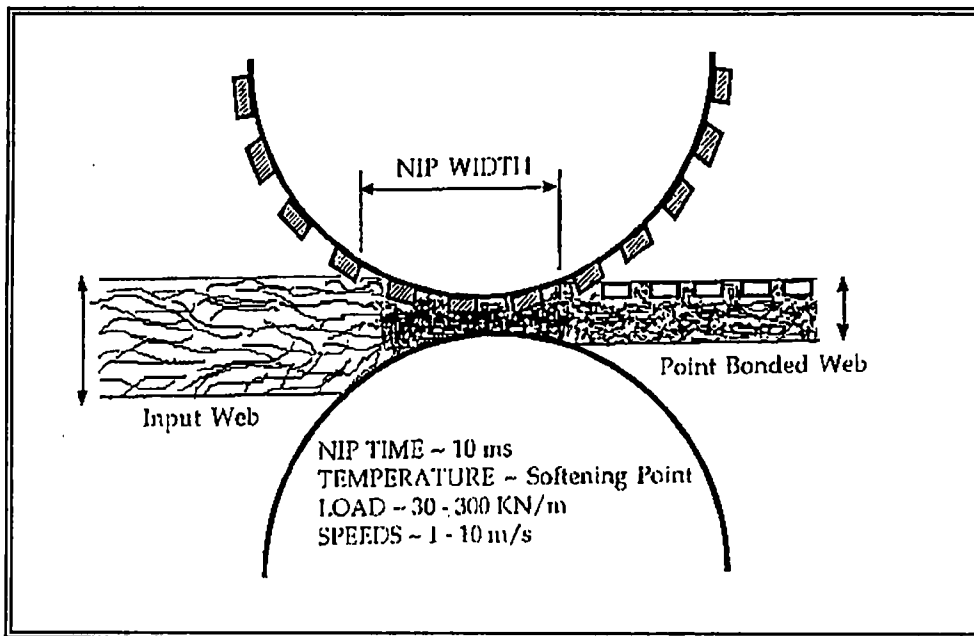
Figure 2.1 Schematic of the Thermal Point Bonding Process

(a) **Heat transfer**: Heat transfer by conduction alone is poor because of low thermal conductivity of polymers. Most favorable estimates show that the temperature at the center of fabric rises up to a temperature roughly 35 °C less than roll temperature. So conduction alone is not responsible for bonding.

(b) **Heat of deformation**: Webs get compressed to approximately 1/10th of their initial thickness at bond points. From SEM studies, bond areas are essentially void free. However, density measurements using a gradient column suggest the void content up to 5%. Warner et al. [10] estimated an upper bound for the temperature rise due to heat of deformation in PP to be 35-40 °C. Part of the heat is probably absorbed in partial melting, so that the actual rise may be lower.

(c) **Clapeyron effect**: The change in melting point of a material under pressure is given by the Clapeyron equation [2]:

$$dP/dT = dH/ (T*dV)$$

where,

P   is the pressure,

T   is melting temperature,

dH is the molar enthalpy of melting, and

dV is the molar volume change on melting.

The above equation indicates that the slope dP/dT is usually positive, because dH/dV is usually positive. This in turn suggests that, as the pressure is raised, the melting temperature will increase. Wunderlich et al. [11] estimated that the melting temperature increase in PP is 38K/kbar. This could lead to a melting temperature increase of about 15K for PP in calender bonding under the lands [10].

8

(d) **Polymer flow**: Flow is important in achieving a good bond, since it helps to encapsulate the fibers, which results in mechanical interlocking of fibers [10]. The flow of the polymer in the nip will be determined by the pressure, the empty volume available, the viscosity and the residence time in the nip.

(e) **Diffusion**: The reptation theory has been used to estimate diffusion distances. The results show that some diffusion occurs. The times and temperatures involved in thermal bonding are insufficient to eliminate the memory of an interface or the fiber integrity. Diffusion distances are of the order of 10s of Angstrom.

The results suggest that flow is more critical to the formation of bond than is diffusion, but this conclusion needs to be supported with experimental data.

2.4 Process-Property Relationship

There are three main process variables, namely bonding temperature, bonding pressure, and time (or calendering speed). Bonding temperature is the most influential parameter followed by pressure and time [3].

2.4.1 Effect of Bonding Temperature

De Angelis et al. [12] measured the dependence of the breaking strength of over-all calendered polypropylene fiber nonwoven fabric on bonding temperature. Their results indicate that, for a given nip-line pressure and calendering speed, the breaking strength reaches a maximum at a critical bonding temperature. On keeping nip-line pressure constant, the critical temperature was found to be a function of the calendering speed. The decrease in breaking strength above the critical temperature level was

attributed to the 'loss of fiber integrity and formation of film-like spots at high temperatures.' Many other investigators [4, 9,13-17] have reported similar results. Gibson and McGill [16] studied the influence of calender temperature on the hand of thermally bonded polyester fiber webs. Lower-temperature-bonded fabrics had a softer hand and were more flexible. Malkan et al. [14] studied failure behavior of polypropylene spunbonded webs with respect to bonding temperature. Brittle failure was mainly associated with higher bonding temperatures and was initiated mainly by bond rupture. Some other researchers [9,16,18] have also reported similar results. The temperature of maximum strength lies in close proximity to surface melting temperature of the fibers [3].

2.4.2 Effect of Bonding Pressure

The influence of the bonding pressure on fabric properties has been investigated by several authors. Results reveal an optimum pressure for obtaining maximum strength, other things being the same. The nip line pressure is important since it influences the heat transfer to and through the web, as well as melting point, flow, and viscosity of the polymer. Bechter et al. [13] found that, in the case of point-bonded polypropylene webs, the bonding temperature at which the strength maximum occurred was unaffected by the nip line pressure. The maximum strength achieved was, however, influenced by the nip line pressure. This influence depends upon melting behavior of the fibers. If the position of maxima occurs in softening region, higher pressure yields higher strength. On the other hand, if maxima occurs in early-melting region, a low calendering pressure is desirable so that the 'thin' melting zone is not disturbed. Muller et al. [19] reported an optimum pressure for the bonding of heavy webs. The author suggested that, at high nip

pressures, flow from the fiber is disturbed and there is considerable fiber damage at the perimeter (as seen through SEM). Both these effects lead to reduction in strength. Crush damage at bond point perimeter has also been reported by Kwok et al. [9].

2.4.3 Effect of Calendering Speed

De Angelis et al. [12] studied the influence of speed on tensile properties of webs. Increasing the speed while maintaining the temperature and pressure constant reduced the breaking strength. Bechter et al. [13] reported somewhat more important conclusions concerning the effect of increasing speed for point-bonded polypropylene webs. As the speed increases, the following things happen:

(a) The calender temperature required for maximum strength increases to compensate for the reduced contact time.

(b) The influence of calendering pressure is greater at faster speeds. The author suggested that this was due to reduced heat transfer at higher production rates.

(c) The maximum strength achieved increases.

An increase in production rate, when compensated by an appropriate increase in temperature, reduced the bond point area and actually increased the fabric strength. Muller et al. [19] also reported an increase in strength with increase in speed.

2.5 What Changes Take Place During Thermal Bonding

Not much work has been done to understand the changes, especially micro-structural, taking place in the fibers in unbonded as well as bonded region during thermal bonding. As the fabric passes through the calender, it gets compressed to approximately

11

one tenth of its original thickness at bond points [10]. As per SEM pictures, bond areas appear void free, although density measurements using a gradient column have suggested void content up to 5%. Many authors [10, 16] have examined optical micrographs and SEM images of bonded areas and reported that fibers' integrity was not completely eliminated in the bond region. However, Drelich et al. [20] studied thermal bonding with fusible fibers and reported that polymer in the bond region no longer has any fiber characteristics.

Scanning Electron Micrographs of bond perimeter showed shear damage of fibers [9-10, 19]. Crush damage at bond perimeter causes sharp reduction in the fiber load bearing ability due to stress concentration at the crush mark. According to Kwok et al. [9], this physical discontinuity in fiber strength along its axis may also be viewed in terms of thermal discontinuity along fiber axis due to difference in heat treatment, melting and recrystallization. They have also analyzed the forms of fiber fracture in broken strips of fabric of high elongation polypropylene and relatively lower elongation Dacron polyester. After examining the fibers in high magnification stereo-scan photographs, they found that approximately 46% of the fibers broke due to fiber damage (crushing), another 48% by pure undamaged tensile failure and the balance were unclear. Surprisingly, both the products showed same distribution. Warner et al. [10] has also reported that a majority of fibers break at bond perimeter with little apparent plastic deformation. The material at the perimeter is weak and brittle. Warner attributed this brittleness to crystallization in an unoriented state, especially at the perimeter where polymer is a result of extrusion from under the pin.

DSC analysis of bond and non-bond areas showed that both bonded and unbonded areas had melting temperatures that were higher than that of polymer. Further, bond areas were more thermally stable than unbonded areas. The influence of pressure on the properties of the polymer in point bonding has been poorly understood. Pressure is expected to increase the melting point and glass transition temperature and thus could exert a significant influence on the rate of crystallization. Pressure also influences the rates of nucleation and crystal growth [2]. Not much is known about the effect of pressure on crystallization of polypropylene. Though Philips and Tseng [21] showed that the volume density of crystal nuclei increases, and high crystallinity level results, when polyester was crystallized under pressure. Malkan et al. [14] studied thermal bonding of polypropylene spun-bonded webs and reported that size and characteristics of bond are not very much affected by bonding temperature and also bonding pressure. However, edges of bond sites become sharper at high temperatures and pressures. On the other hand, Wei et al. [4] have reported that bond area increases with increase in bonding temperature. They also reported shrinkage of fibers during thermal bonding especially in the case of highly drawn fibers.

It is clear from above review that structural changes taking place in the fibers during the thermal bonding operation need to be properly understood, and that was one of the main objectives of this research.

2.6 Polypropylene Fiber Structure and Morphology: Effect of Spinning and Drawing Conditions [22]

2.6.1 Spinning

On the basis of the most accepted model of fiber structure, spun PP fibers may be considered to consist of two phases: an amorphous and a crystalline phase [23-24]. The crystalline phase is composed of discrete lamellae or crystallites. The lamellae, each consisting of many chain folded molecules, are connected by tie molecules, which make up part of the amorphous phase. Other molecules in amorphous region are those whose tacticity or molecular weight difference prevents their crystallization. In addition, portions of some molecules exist in disordered fold regions on the surface of crystal. Even within the crystals, imperfections and disorders exist, and these regions contribute to the amorphous content. The crystallites and amorphous regions exist together in larger, complicated structures. Quiescent melt crystallizes in clusters of spherulites. The spherulites form around a nucleus, which is a chance alignment of molecular chain segments that causes crystallization to begin. When melts solidify under the condition of sufficient high stress, as fibers usually do, a different aggregation of crystalline and amorphous regions arises. Instead of point nucleation, row nucleation occurs, and lamellae grow epitaxially along fibrillar molecular structures. This gives rise to the so-called 'shish-kebob' structure. The exact nature of the aggregates depends upon tacticity, molecular weight, molecular weight distribution, additives and spinning conditions.

Ziabicki [25] has given an extensive review of melt spinning process. The properties of spun PP fibers are determined by the stress existing in the spin line at the position of final diameter, at least at moderate spinning speeds. The stress level is largely determined by:

1. Take-up velocity

2. Molecular weight

3. Extrusion temperature

4. Extrusion speed

5. Air cross-flow rate and temperature

Hagler [26] has given a simple method for estimating qualitatively the effects of various spinning parameters on spin line stress and consequently the properties of the spun fiber. The stress is related to how fast the spin line is stretched and cooled, not how much draw-down occurs in the spinning process. Draw-down (draw ratio) is important for drawn fibers, where the time constant of relaxation is much larger.

Several authors [27-34] have studied the effects of spinning conditions on the basic fiber properties of spun PP fibers. Nadella et al. [34] studied PP with a broad range of melt flows. In all of their air-quenched filaments, only the monoclinic crystal form was produced. In monoclinic form, the chains are helices with axes lying along the c-axis. The crystallization was observed to occur in the spin line, and during the crystallization, the birefringence rose rapidly. C-axis (a, b, c are crystal axes; a' axis is perpendicular to b and c axes) orientation was observed to increase with spinning speed. An increase in orientation was also obtained with an increase in molecular weight. These authors found a pronounced effect of extrusion temperature on the orientation of the spun fibers. Increasing the spinning temperature resulted in a lower orientation. In rapid quenching, such as spinning in to ice water, PP crystallizes in paracrystalline (smectic) form. Henson and Spruiell [32] have shown that the degree of crystallinity increases as the spin line stress increases. The value of the crystalline orientation function (f_c) increases with stress until the c-axis is nearly aligned with fiber axis. The b-axis quickly aligns perpendicular to the fiber axis. The $f_{a'}$ values decline slowly at first, but then approach −0.43.

Birefringence increases with increase in spin line stress. The orientation developed in the crystalline regions is always greater than that developed in the amorphous regions. Shimizu et al. [35] have studied the spinning of 9 MFR PP at speeds up to 7000 m/min. The rate of increase of birefringence with respect to take-up speed decreases with increase in take-up speed.

PP exhibits a distinctive bimodal orientation of the unit cells when crystallized from melts undergoing extension. There are crystals whose c-axis is oriented parallel with the fiber axis and a smaller population of crystals whose a'-axis is oriented parallel with the fiber axis. Nadella et al [33] estimated the percentage of these crystals to be about 10-20, at high stress. Anderson and Carr [31], and, Clark and Spruiell [36] concluded that the a'-axis-oriented crystals are very small and are distributed throughout the sample and perhaps grow epitaxially to the c-axis-oriented crystals.

Minoshimo et al. [37] predicted, on the basis of data taken at very low take-up speeds, that narrow molecular weight distribution resins would yield spun fibers with more orientation than broader molecular weight distribution resins. The data suggested that the apparent elongational viscosity in spinning may be higher at moderate to high extension rates for the narrow molecular weight distribution materials. The higher viscosity, it was predicted, will give higher spin line stresses and thus higher degrees of orientation. Fung et al. [29] measured birefringence in 10 microns sections of PP fibers. They found that the birefringence was higher near the surface of the fibers. These higher birefringences have been postulated to be due to the rapid cooling on the outside and the consequent increase in viscosity and load bearing in outside layers.

2.6.2 Drawing

On a macroscopic scale, drawing seems to be a simple process. However, on a microscopic scale, profound changes occur in the fiber structure. Deformation and rearrangement of the morphological structure have been described by Peterlin et al. [38-40] and Samuels et al. [24]. During the initial step of deformation, a crystalline fiber goes through an affine deformation, i.e., the strains are uniform throughout the material. However, even at still small deformations the morphological inhomogeneity of the lamellar structure and the small resistance of the lamellae to the plastic shear deformation lead to shear, tilt, rotation, and separation. Lamellae parallel to the applied stress may deform in a different manner from lamellae perpendicular to the stress.

With sufficient deformation, lamellae are broken up into folded chain blocks approximately 20 nm in width. These blocks subsequently aggregate to form the basic units of the drawn fiber- the microfibril. The microfibrils consist of alternating blocks of folded-chain crystals and amorphous regions that are mostly chain folds. Another essential part of the amorphous region are the tie molecules that connect the blocks in the fiber axis direction and provide the major source of resistance to deformation and strength of the fiber. The tie molecules are believed to be located mainly on the surface of microfibrils and to extend along many crystal blocks. The microfibrils are aggregated laterally to form the fibrils.

The microscopic deformation described above can proceed macroscopically in two different ways. The fiber may deform uniformly, or it may deform by the well-known necking process. The mode of deformation depends on the properties of the spun fibers and conditions of drawing. Shimizu et al. [35] found that fibers spun at speeds

higher than 3000 m/min did not exhibit necking when drawn. Nadella et al. [41] also found that the tendency to form necks was reduced in fibers spun under high spin line stress.

Ziabicki [25] showed the effects of temperature on mode of deformation. With increase in temperature, plastic flow becomes more and more pronounced. Nadella et al [40] studied drawing of PP at both ambient and 140 °C temperatures. Samples of cold-drawn fibers were subsequently annealed at 140 °C for 15 min. As was expected, drawing increased the crystalline orientation in all cases. Rate of increase of birefringence with respect to draw-ratio decreased with increase in draw-ratio. The higher the as-spun orientation, the lower was the draw ratio necessary to develop a given higher level of orientation. In both the hot-drawn, and the cold-drawn and annealed fibers, the orientation of a'-axis gradually disappeared. Densities of drawn samples were higher than those of the spun fibers. Crystalline fraction as high as 61% was observed. Based on small angle X-ray studies, it was concluded that cold-drawing disrupts the entire structure including the unit cell as well as the morphological units. Hot drawing was viewed as causing a less severe disruption of the structure than cold drawing. Kitao et al. [42], in comparing similar cold-drawn fibers and hot-drawn fibers, found that the density of the cold-drawn fiber decreased significantly with draw ratio. The density of the hot-drawn fibers remained essentially constant.

Sakthivel et al. [43] conducted a study of polypropylene spinning and drawing under commercial conditions. The fibers were spun at 500, 1000, and 2000 m/min. The fibers which were drawn were spun at 2000 m/min. Strong dependence of fiber structure on spinning and drawing conditions were reported.

2.7 Polypropylene Annealing and Melting Behavior

Although the residence time of the fibers in the thermal bonding process is not sufficient to anneal the fibers properly, there should be some effect. Annealing the fibers quickly releases the stress, heals the voids and structural defects, and leads to increases in degree of crystallinity, and perfection and size of crystallites. If heated with free ends, the annealing causes the fiber to shrink. Balta-Calleja et al. [44] investigated annealing phenomena of drawn polypropylene fibers. They found that the relaxation of tie molecules, shrinkage, and disorientation proceeded relatively fast, compared with the long period growth and the increase in density.

Jaffe et al. [45] studied melting behavior of spun fibers produced at different spin-line stress levels. He reported the presence of the high temperature shoulder on the main melting peak of the high-stress sample. Jaffe attributed the high melting shoulder to the melting of the fibrillar crystal nucleating species of the row structure. Multiple melting peaks have been also reported by Samuels [46]. He also reported that the endotherms occur at higher temperatures the more the fibers are drawn. Katayama et al. [47] have shown that, in spun fibers the a'-axis-oriented crystals melt at a temperature lower than the melting temperature for the c-axis-oriented crystals.

2.8 Role of Fiber Morphology in Thermal Bonding

Although the effect of fiber structure was considered very important in determining the properties of nonwovens, the role of fiber morphology in point bonding and the changes taking place during the process have not been examined. So far most of

the work has been done to understand the effects of bonding conditions on fabric properties. Some work [3-5] has been done on the effect of fiber properties on final fabric properties. Morphological changes taking place in the fibers due to thermal bonding have been almost untouched.

Wei et al. [4] studied the effect of fiber draw-ratio on PP nonwoven fabric properties. Fibers with lower draw-ratio resulted in fabric with higher tensile strength and lower flexural rigidity. Shrinkage during thermal bonding was reported to be higher for higher draw-ratio fibers. Also, they emphasized that nonwoven fabric properties are primarily determined by the bonding regions, and to a lesser extent by constituent fiber properties. Bechter et al. [3] studied the properties of the polypropylene webs and reported that the type of polymer and the spinning conditions have a considerable influence on the tensile strength of calendered polypropylene nonwovens. A lower degree of drawing of fibers led to markedly higher strength in nonwovens. Wyatt et al. [5] studied thermally bonded PET webs with binder fibers. They reported that base fibers having higher crystallinity and orientation generally exhibit higher fabric rigidity as well as breaking strength.

Zhang et al. [48] studied evolution of structure and properties in the spunbonding process. The studies showed that fiber morphology plays an important role in bond formation. The nature of bond points depends on fiber morphology. In addition, they reported that smaller diameter fibers with higher birefringence resulted in better tensile properties of calendered webs. However, difference in tensile properties for the fabrics was not as large as for the fibers. They also studied effects of free and fixed length annealing and reported a considerable change in the structure and properties of the fibers

20

during annealing. However, annealing might not be a proper simulation of calendering conditions.

From this discussion, it is clear that there is a need of inventive research to examine the changes taking place during thermal bonding and to study the role of fiber morphology in it.

2.9 Web Structure and Properties

Web properties depend not only on the properties of individual fiber but also how the fibers in the web share the stress during deformation. The latter is primarily governed by web structure. A lot of work [49-52] has been done to predict the tensile properties of the webs in terms of the web structure (fiber orientation distribution) and the fiber stress-strain properties. In all the cases, the difference between predicted and experimental stress-strain curves of webs was wider at higher strain levels. It was because, at higher strain levels, the nature of failure of the bonds and their strength also contributes significantly to the stress-strain curve. Whereas, at low strains, it is only deformation of fibers which is important. Therefore, it becomes equally important to understand the behavior of fibers in the unbonded region, bonded region, and bond vicinity.

2.10 Spunbonding

2.10.1 Process Description

Spunbonding is a one step unique process, which involves fiber extrusion, fiber attenuation, web formation, and bonding of web to impart strength, cohesiveness, and integrity to it. The filament spinning, drawing, and deposition are the most critical steps

in the spunbonding process. Hartman et al. [53] proposed some of the various basic possible variations of the process, which are shown in Figure 2.2.

The first process (A) uses longitudinal spinnerets, with air slots on both sides of the spinneret for the expulsion of drawing air[1]. The room air[2] is carried along and after lay-down of the filaments is removed by suction[3]. This process is very well suited for tacky polymers, such as polyurethane. Bonding takes place due to tackiness of the filaments.

The second process (B) allows a higher draw-ratio, with subsequently increased orientation of the filaments. Filaments are drawn with several air or gas streams[1], [2], &[3] using drawing conduits. The air is removed by suction[4] after web formation. This process has special advantage in preparing fine spunbonded webs with a textile-like appearance and handle of the web.

The third process (C) operates with regular cooling ducts[1] and drawing jets[3]. The drawing and cooling arrangements can be operated to give very high spinning speeds. The temperature and humidity of room air[2] can be controlled. The air is removed by suction[4] after web formation.

The fourth process (D) has a mechanical drawing step between spinneret and lay-down zone. A very high level of molecular orientation can be achieved with this method. Rest of the process is similar to process (C).

A number of spunbonding processes can be classified into one of the above basic four types of the process. The method of bonding may be chemical, mechanical, or thermal. Thermal bonding is the most widely used technique for spunbonding.
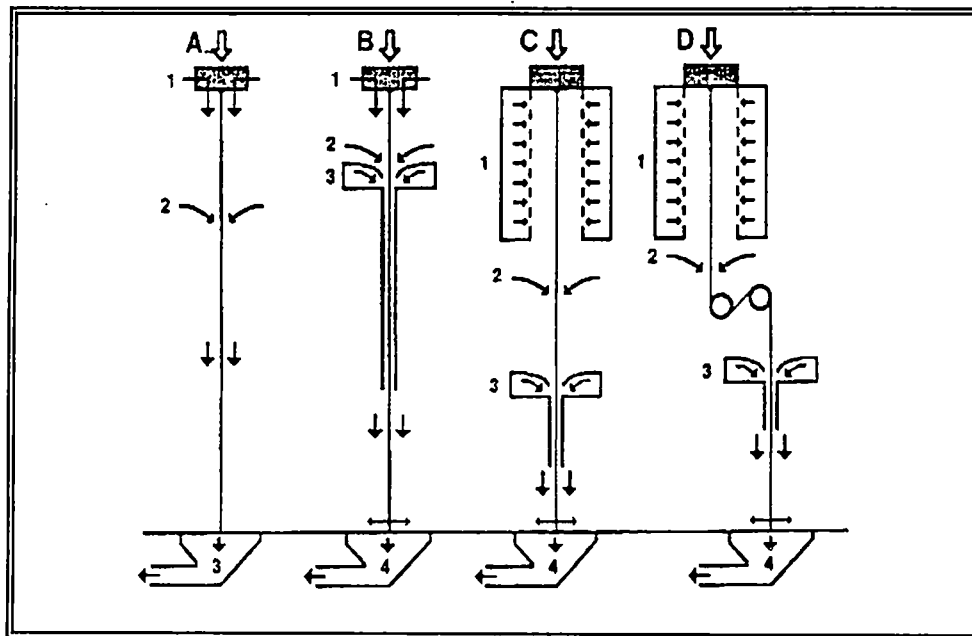
Figure 2.2 Four Basic Variations of the Spunbond Process

Reicofil® system shown in Figure 2.3 has been developed by Reifenhauser GmbH of Germany. The polymer pellets are fed into the extruder hopper. Polymer is melted and mixed as it moves along the extruder. The molten polymer is delivered to metering pump, which in turn feeds the polymer to spinning block at a constant rate through a feed distribution system. The feed distribution, which is very critical, balances the flow, the temperature and the residence time of polymer across the width of the die. The spinneret, which is rectangular in shape, has several thousands of holes. The cooling air-duct, located below the spinning block, continuously cools the filaments with conditioned air. Air is sucked away at the bottom by a ventilator. The filaments are drawn and laid-down on a moving sieve belt simultaneously by venturi effect. The condensed web passes over moving belts and is thermally bonded by hot calenders. The bonded web is then wound under slight tension.

2.10.2 Process-Structure-Property Relationship

Malkan et al. [14-15] investigated the effect of processing parameters on fabric properties in the Reicofil® spunbond process. The variables studied were polymer throughput rate, melt temperature, primary air temperature, airflow rate, bonding temperature, bonding pressure and production speed. Polymer throughput rate and bonding temperature had the most significant effect on web properties. The final fiber diameter was thought to be an important resultant variable in controlling many key properties of spunbond webs. The final fiber diameter was shown to decrease with an
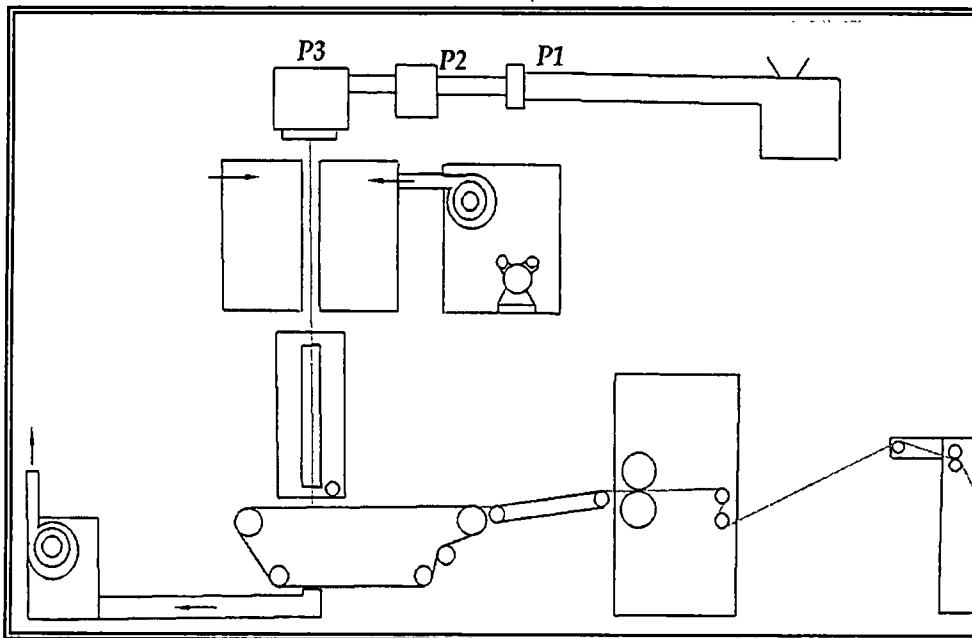
Figure 2.3 Schematic of Reicofil-II Spunbond Line

increase in cooling air temperature and melt temperature, and with a decrease in polymer throughput rate.

Spruiell et al. [54] investigated the spunbonding process (Reicofil®) using a mathematical model. The model was applied to investigate the effects of various polymer and process variables on the resulting filament structure and properties. The material parameters studied were polymer elongational viscosity and the kinetics of stress induced crystallization. The process parameters included the extrusion temperature, mass throughput rate, spin-line length, cooling air temperature, airflow rate, and the shape of the draw-down venturi. The model indicated that the elongational viscosity is a key factor in controlling the amount of draw-down, the temperature at which crystallization occurs and the level of molecular orientation achieved. The polymer crystallization kinetics also has a major influence on the temperature of crystallization but relatively little effect on the filament draw-down. Of the process parameters, cooling air temperature and airflow rate were found to be the most critical. The model predicted that the fiber diameter, crystallinity, and birefringence decreased with an increase in cooling air temperature.

Zhang et al. [48] also did fundamental investigation of the Reicofil® spunbond process using both a polypropylene homopolymer and a polypropylene copolymer. The study showed that primary air temperature and throughput rate had the most significant effect on filament and bonded web properties. There was a decrease in fiber diameter with decrease in throughput rate and cooling air temperature. The decrease in fiber diameter was accompanied by an increase in their crystallinity, birefringence, tensile strength, initial modulus, thermo-mechanical stability, and density. X-ray diffraction studies showed that crystal orientation increased with a decrease in primary air

26

temperature. Also, the investigation showed that there exists a strong relationship between the structure and properties of filaments and the properties of nonwoven fabrics. However, difference for properties of fabrics was not as large as for properties of filaments.

CHAPTER III

EXPERIMENTAL DETAILS

3.1 Processing

3.1.1 Staple Fiber Webs

Fiber grade polypropylene, which had a melt flow rate of 17 dg/min, supplied by Montell USA Inc., was used for the production of the fibers. The fibers were produced on the Fourne extruder & spinning setup, a schematic of which is shown in Figure 3.1, using a seven-hole die with hole diameter of 0.764 mm and L/D ratio of five. Extruder screw size was 300 mm × 13 mm. The height from spin-pack to winder was 3 m. The extrusion temperature was kept constant at 230 °C. Polymer throughput rate and takeup speed were varied in order to achieve the same final diameter for all the fibers. Ambient air was used as quenching medium. Out of six samples produced, three were as-spun with no drawing and three were drawn after spinning. Drawing was done at 140 °C on a two-stage conventional drawing machine with heated rolls (manufactured by Fincor Incom Inc.). The temperatures of first rolls and third rolls were 50 °C and room temperature, respectively. The draw ratio in first zone was kept constant at 1.10. The draw ratio in the second zone was set to obtain the desired final diameter. The details of all the fiber samples are summarized in Table 3.1.

The continuous filaments were chopped into staple fibers of length 40 mm for carding. Chopped staple fibers, with an appropriate level of water (10 %) and LUROL PP-8049 spin-finish (0.4 %) supplied by Goulston Technologies, were carded on a Saco-

28
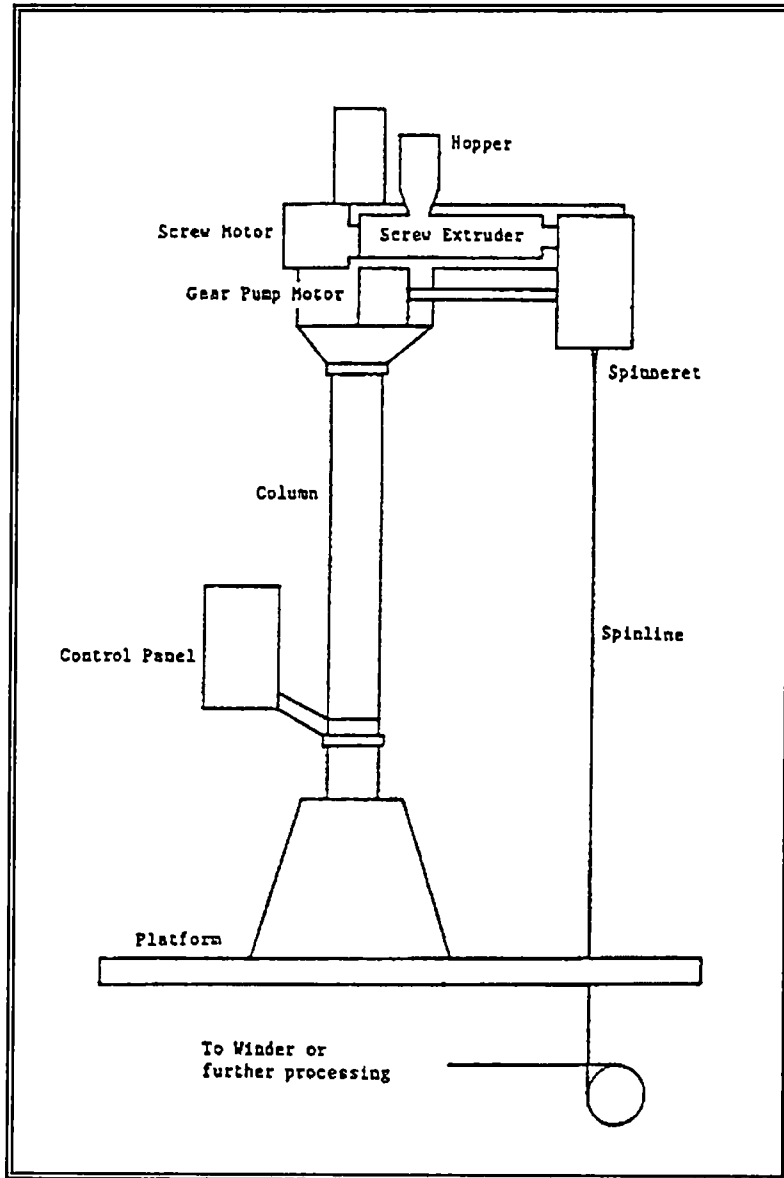
Figure 3.1 Schematic of Fourne Melt-Spinning Setup

Table 3.1 Details of the Fiber Samples Produced

SAMPLE ID	POLYMER THROUGHPUT RATE (G/HOLE/MIN)	NOMINAL SPINNING SPEED (M/MIN)	DRAW RATIO	DENIER
As-spun 1	0.281	1000	Undrawn	2.70
As-spun 2	0.410	1500	Undrawn	2.50
As-spun 3	0.554	2000	Undrawn	2.50
Drawn 1	0.420	1000	1.50	2.40
Drawn 2	0.716	1000	2.50	2.70
Drawn 3	0.963	1000	3.50	2.40

Lowell carding machine to produce webs with a nominal basis weight of 40 g/m². Carded webs were then bonded at five-six different bonding temperatures and at a speed of 5 m/min using a Kuster point-bonding calender having 15 % bonding area. Speed was kept low due to difficulties in handling of small carded webs. Nip pressure was kept constant at 350 pli for all the samples.

3.1.2 Spunbond Webs

Spunbonding studies were carried out using 35 MFR EXXON PP on the Reicofil-II spunbonding line at the University of Tennessee, Knoxville. Schematic of the process variables is shown in Figure 3.2. Melt temperature and cooling air temperature were the main variables. Airflow rate was adjusted to achieve the same fiber diameter for all three sets. Webs were bonded at four different bonding temperatures for each set of fibers. Other process parameters such as bonding speed and calender pressure were kept constant. Filament samples before bonding were also collected for analysis.

3.2 Characterization of the fibers and the webs

3.2.1 Tensile Properties

Tensile properties of the fibers and fabrics were measured using the United Tensile Tester with test conditions described in the ASTM D3822-91 for filaments and ASTM D1117-80 for nonwoven fabrics [55]. However, for fiber samples, a gauge length of 2" (5.08 cm) and an extension rate of 10"/min (25.4 cm/min) were used. The spunbond filaments were carefully separated from unbonded webs avoiding any deformation of the sample during that process. The sample was then mounted in a paper window under

```
                    ┌─────────────────────────────┐
                    │        PP (35 MFR)          │
                    │  Throughput  0.4 g/h/min    │
                    │  Basis weight  35 gsm       │
                    │  Belt Speed  42 m/min       │
                    └─────────────────────────────┘
              ┌──────────────────┼──────────────────┐
    ┌──────────────┐    ┌──────────────┐    ┌──────────────┐
    │    SET I     │    │    SET II    │    │   SET III    │
    │ Melt temp    │    │ Melt temp    │    │ Melt temp    │
    │   210 C      │    │   230 C      │    │   250 C      │
    │ Air temp 15 C│    │ Air temp 20 C│    │ Air temp 25 C│
    └──────────────┘    └──────────────┘    └──────────────┘
```

Webs were bonded at four different bonding temperatures for each of the sets
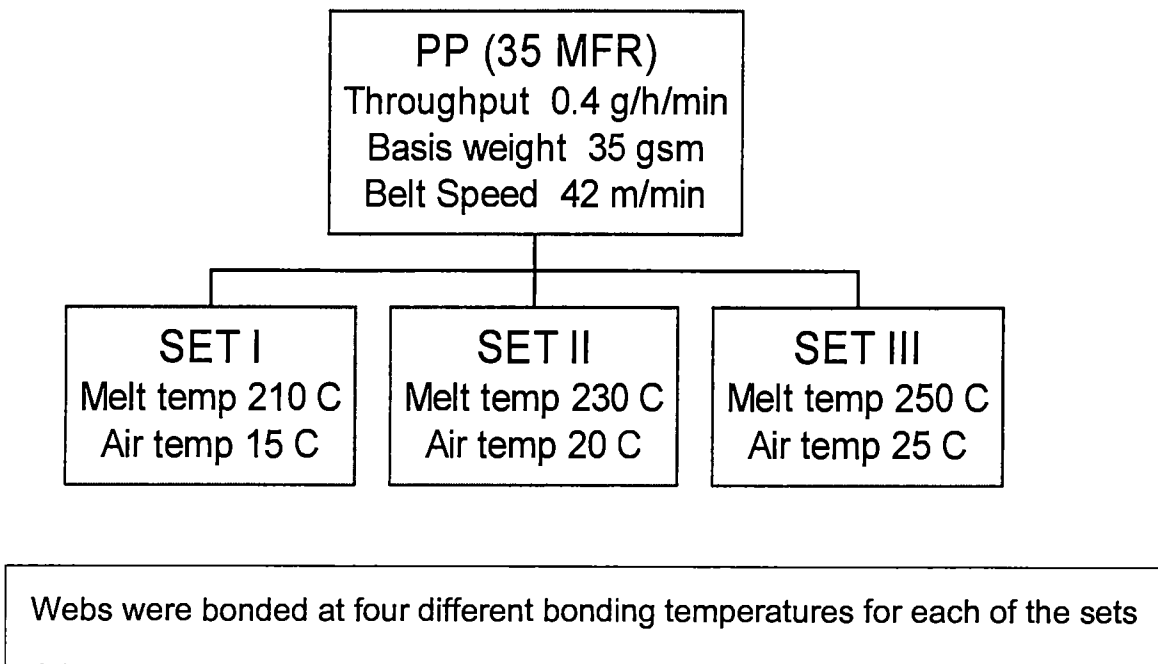
Figure 3.2 Schematic of Spunbond Process Variables

slight pretension for further testing. For webs, a gauge length of 5" (12.7 cm), width of 1" (2.54 cm), and extension rate of 5"/min (12.7 cm/min) were used in both machine direction and cross direction. Carded webs were tested only in machine direction due to insufficient width of the webs.

3.2.2 Single-Bond Strip Tensile Test

This test was developed in-house and was done in order to estimate bond strength and the degree of load sharing between the fibers during tensile deformation of the web. A schematic of this test is shown in Figure 3.3. A tiny strip of size 80 mm × 5 mm was cut from the web. The strip was cut across the width direction from two sides to leave only one bond uncut in the middle of the strip, as shown. The strip was then subjected to a conventional tensile test. The test was conducted on the United Tensile Tester with a gauge length of 1" (2.54 cm) and extension rate of 0.5"/min (1.27 cm/min). A total of twenty tests were done for each sample.

3.2.3 Differential Scanning Calorimetry

Differential Scanning Calorimetry of the fibers, fabrics and only-bonds was done using a Mettler thermal analysis system consisting of TC 11 controller and DSC25. The scans were done at a heating rate of 10 °C/min in air. Crystallinity of the samples was calculated from the enthalpy of melting (ΔH) determined from the scans. ΔH value of 190 J/g for 100 % crystalline polypropylene was used for estimating the crystallinity of the samples [56]. Bonds were separated carefully from the web using a sharp pair of scissors.
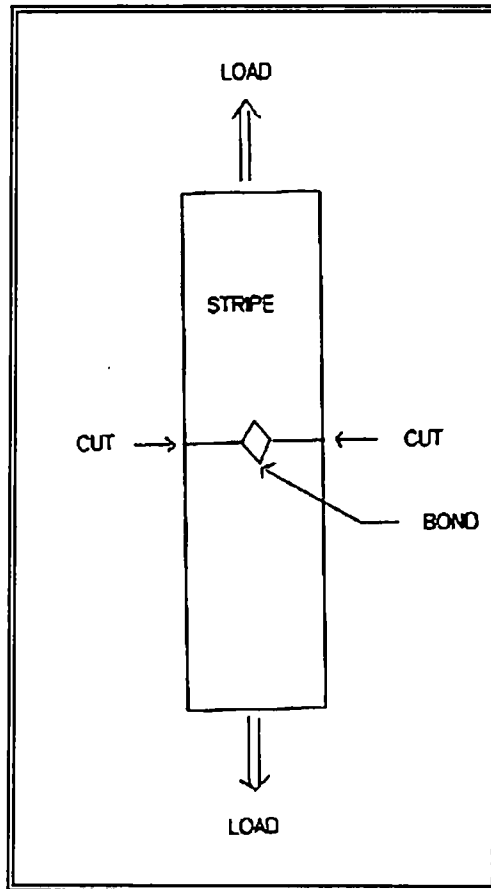
Figure 3.3 Schematic of Single-Bond Strip Tensile Test

3.2.4 Thermomechanical Analysis (TMA)

Thermomechanical responses of the fibers were recorded using the Mettler thermal analysis system consisting of TC11 controller and TMA40. The scans were obtained at a heating rate of 10 °C/min in air. A test length of 10 mm was used. The samples were held by copper clips at both ends, and a constant load was applied during the scan. The test was done under low as well as high tension for a given fiber sample.

3.2.5 Denier

The fiber denier was determined by measuring the mass of a known length of the fiber and then the mass converted to that of 9000 meters of length to be expressed as denier.

3.2.6 Diameter and Birefringence

Fiber diameter and birefringence were measured using an optical microscope. The retardation technique was used for measurement of birefringence. For unbonded regions of the web, fibers in that region were cut and separated from the web using a sharp pair of scissors. Thirty measurements were taken in all the cases.

3.2.7 Estimation of Molecular Orientation in Bonds

It is not possible to measure molecular orientation in bonds in terms of birefringence. An alternative method was developed in-house to compare the molecular orientation in bonds for different fibers. Bonds were carefully separated from the web

using a sharp pair of scissors. Four sides of bond were measured under a microscope. Bond was placed in a DSC pan and heated up to 160 °C using Mettler DSC25 at a rate of 10 °C/min. Four sides of bond were again measured after the sample cooled down. Percentage linear shrinkage in bond was calculated and was considered as a measure of molecular orientation. The higher the shrinkage, the higher the molecular orientation. Five tests were done for each sample.

3.2.8 Wide Angle X-ray Diffraction (WAXD)

X-ray diffraction photographs for staple as well as spunbond fibers were obtained using a Phillips Electronics x-ray diffractometer at 35 kV and 15 mA. The exposure time was five hours. Sample was prepared as a parallel bundle of fibers. The wavelength of x-ray was 1.54 A° in all the x-ray studies. Crystalline and amorphous orientation functions were determined from azimuthal scans using the Rigaku WAXD system in transmission mode, crystallinity, and birefringence. Azimuthal scans were done on parallel bundle of fibers at $2\theta = 13.7°$ and $16.5°$, at a rate of 2 °/min. Crystallite size was measured using the Rigaku WAXD system in reflection mode. Crystallite size was calculated automatically by the computer from full width half maximum of reflection peaks in equatorial scans [57]. Equatorial scans were done from $2\theta = 10°$ to $30°$ at a step of $0.01°$ and dual time of 4 seconds. "Duco Cement" was used as a glue for sample preparation for equatorial scans. Use of Duco Cement was helpful in sample preparation from only-bonds and very short fibers from unbonded regions of the web. Duco Cement is totally amorphous and does not interfere with crystalline peaks of polypropylene. The Rigaku

WAXD system was operated at 35 kV and 30 mA. Here also, bonded and unbonded regions were carefully separated from the web using a sharp pair of scissors.

3.2.9 Bursting Strength

Bursting strength of the webs was measured on the Mullen Tester using INDA standard test method IST 30.0-70(R82) [58]. Ten measurements were taken for each sample. Bursting strength was measured only for spunbond webs.

3.2.10 Scanning Electron Microscopy

SEM images of the fabrics and the tested samples were taken using a Hitatchi S-3000N electron microscope. Back-scattered images under 30 Pa gas pressure were taken in order to minimize the problems due to static charge generation. Images were obtained in the magnification range of 100 to 1500x.

3.2.11 Density Measurement

A density gradient column was used to measure the density of the fiber and fabric samples. The two solvents used were isopropanol and ethylene glycol. The density range of the column was 0.87 to 0.92. Three measurements were taken for each sample. Density was measured for spunbond fibers and webs only, where the differences in crystallinity were marginal and were difficult to be detected from DSC analysis. Crystallinity of the sample was calculated using the following formula [59]:

$$\text{Crystallinity (\%)} = [\rho_c(\rho-\rho_a)/\rho(\rho_c-\rho_a)]*100$$

Where: ρ = Measured density

ρ_c = 0.938 g/cm^3 [60], Density of 100 % crystalline PP

ρ_a = 0.852 g/cm^3 [60], Density of 100 % amorphous PP

3.2.12 Melt Flow Rate (MFR)

The melt flow rates of the resin as well as the fabric samples were measured using the Extrusion Plastometer. MFR was measured at 230 °C temperature and 2.16 kg load. An average of two measurements is reported.

3.2.13 Fiber Orientation in the Webs

Fiber orientation in the webs was measured using the Webpro$^®$ image analysis system at the University of Tennessee, Knoxville. Orientation ratio, the ratio of the number of the fibers in the machine direction to that in the cross direction of the web, was reported.

3.2.14 Statistical Analysis

Statistical analysis was done using the 'Analysis of Variances' method, the ANOVA procedure in SAS. Statistical analysis was done only for spunbond studies where the differences were relatively small. Three null hypotheses were tested:

1. There were no differences in the mean fiber tenacity for Set I, Set II and Set III fibers.

2. There were no differences in the mean web strength for Set I, Set II and Set III at all the bonding temperatures.

3. There was no significant effect of bonding temperature on web strength.

CHAPTER IV

RESULTS AND DISCUSSION

4.1 Staple Fiber Studies

4.1.1 Staple Fiber Properties

Fiber properties are listed in Tables 4.1, 4.2 & 4.3. DSC scans are shown in Figure 4.1. Thermomechanical (TMA) responses of the fibers are shown in Figure 4.2. WAXD photographs are shown in Figure 4.3. The six fiber samples covered a very wide range of orientation, crystallinity, crystallite size and other morphological aspects. Fiber diameter was within the targeted range in all the cases. Fiber diameter was intentionally kept the same so that the differences due to change in diameter could be minimized and the role of fiber micro-morphology in thermal bonding could be analyzed. As can be expected, there was an increase in molecular orientation and crystallinity of the fibers with increase in spinning speed and draw ratio. Both crystalline as well as amorphous orientation functions improved with increase in spinning speed and draw ratio. TMA and tensile data also supported the morphological differences between the fibers. Fibers with higher molecular orientation and higher crystallinity showed higher strength and lower breaking extension. Shrinkage in fibers, determined from TMA under low tension, with increase in temperature related very well with molecular orientation of the fibers. Fibers with relatively more developed morphology, i.e. higher molecular orientation and higher crystallinity, showed higher thermo-mechanical stability.

39

Table 4.1 Fiber Morphological Parameters

SAMPLE ID	DIAMETER (μM)	BIREFRINGENCE (X ×10⁻³)	CRYSTALLI-NITY (%)	F_C	F_{AM}	CRYSTAL SIZE (A°)
As-spun 1	20.8	19.0	36.7	0.4287	0.3797	140
As-spun 2	19.5	20.4	41.3	0.5586	0.3897	185
As-spun 3	19.7	17.8	45.0	0.4810	0.3479	150
Drawn 1	19.9	23.8	48.9	0.6809	0.4596	140
Drawn 2	20.7	29.4	53.7	0.7361	0.6435	155
Drawn 3	19.5	31.4	56.4	0.7837	0.7070	135

Table 4.2 Fiber Thermomechanical Properties

SAMPLE ID	TMA SHRINKAGE (%)	TMA FAILURE TEMP. AT LOW TENSION (°C)	TMA FAILURE TEMP. AT HIGH TENSION (°C)
As-spun 1	Nil	142	79
As-spun 2	1	142	124
As-spun 3	12	146	128
Drawn 1	10	146	134
Drawn 2	24	156	150
Drawn 3	27	156	152

Table 4.3 Fiber Tensile Properties

SAMPLE ID	TENACITY (GPD)	BREAKING EXTENSION (%)
As-spun 1	2.9	290
As-spun 2	4.8	280
As-spun 3	6.4	190
Drawn 1	6.4	160
Drawn 2	7.4	60
Drawn 3	8.5	25
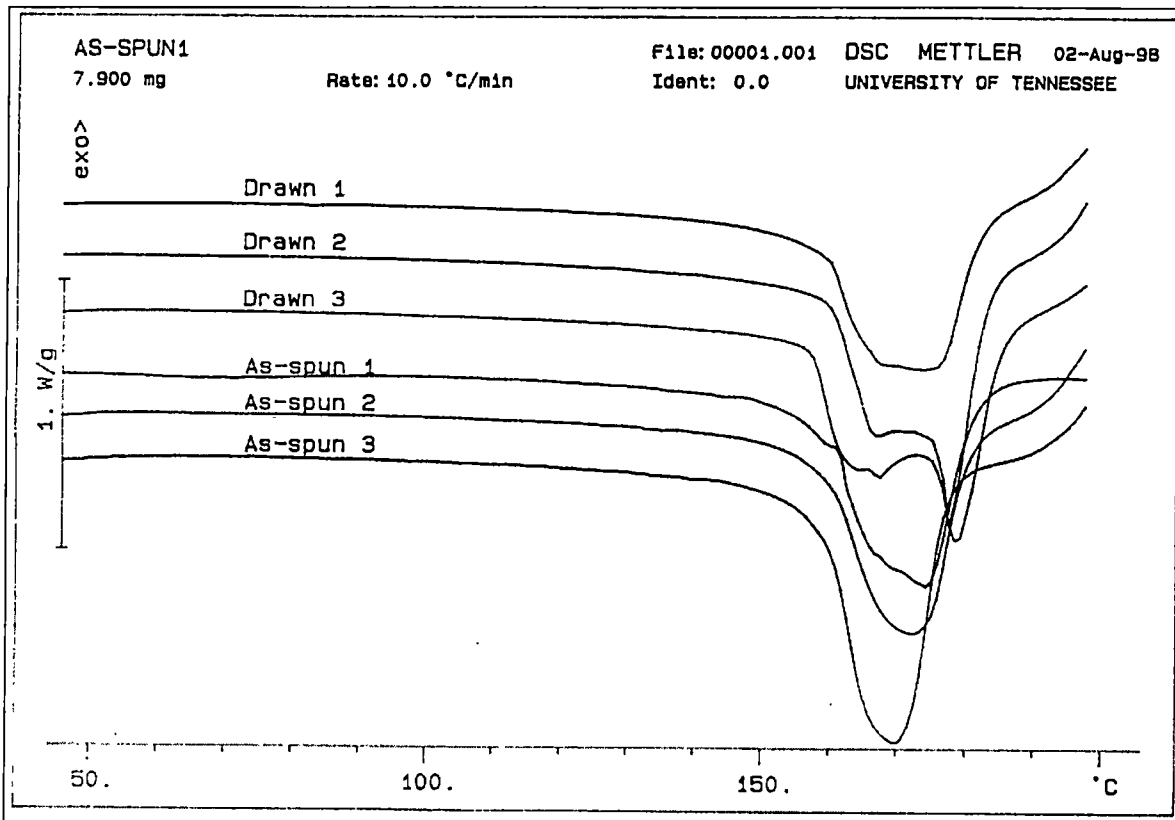
Figure 4.1 DSC Scans of Staple Fibers

DRAWN, 6 0.005N/7
10.000 mm   Rate: 10.0 °C/min

File: 00027.001   TMA   METTLER   10-Aug-98
Ident: 0.0   UNIVERSITY OF TENNESSEE

μm

2000.

Drawn 3
Drawn 2
Drawn 1
As-spun 3
As-spun 2
As-spun 1

50.   100.   150.   °C
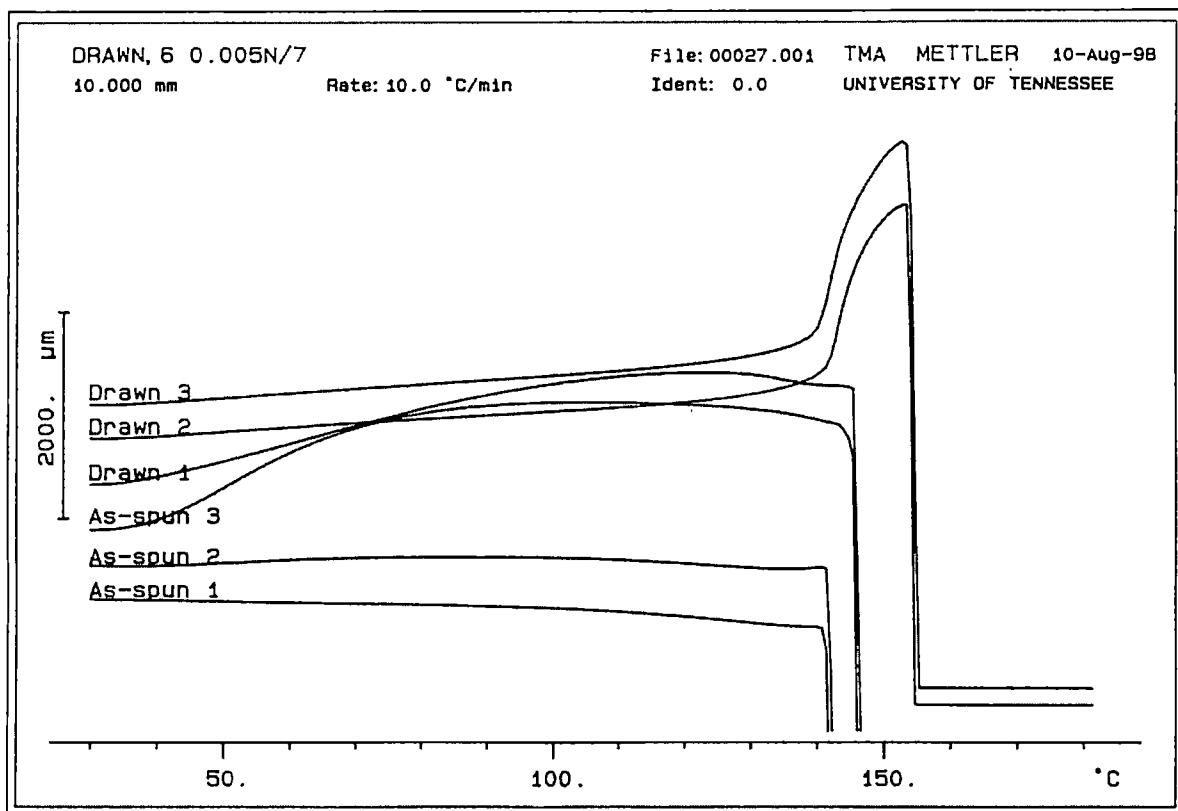
(a)

Figure 4.2 Thermo-mechanical Responses of Staple Fibers Under Low (a) and High
          (b) Tension

43

Drawn, 4   (0.05N/7)   File: 00023.001   TMA   METTLER   10-Aug-98
10.000 mm   Rate: 10.0 °C/min   Ident: 0.0   UNIVERSITY OF TENNESSEE

Drawn 3
Drawn 2
Drawn 1
As-spun 3
As-spun 2
As-spun 1

5000. μm

50.   100.   150.   °C
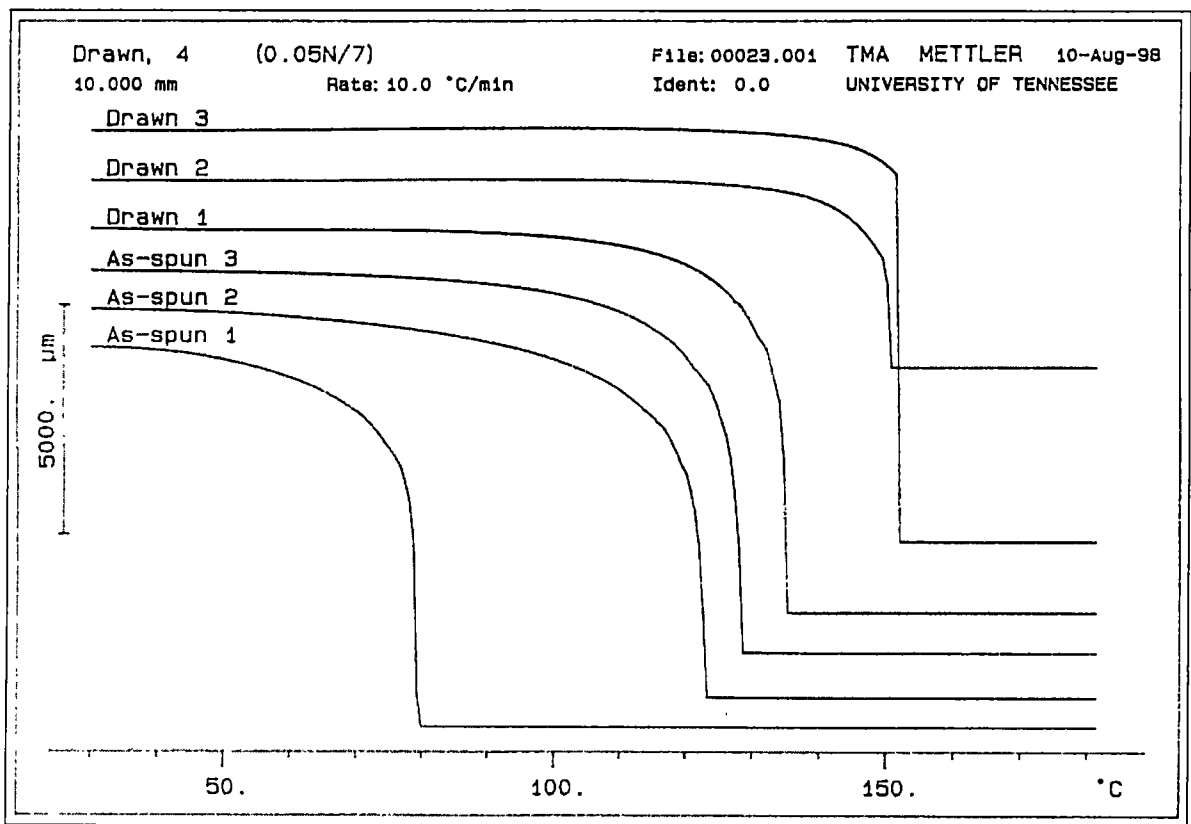
(b)

Figure 4.2 (Continued)

44
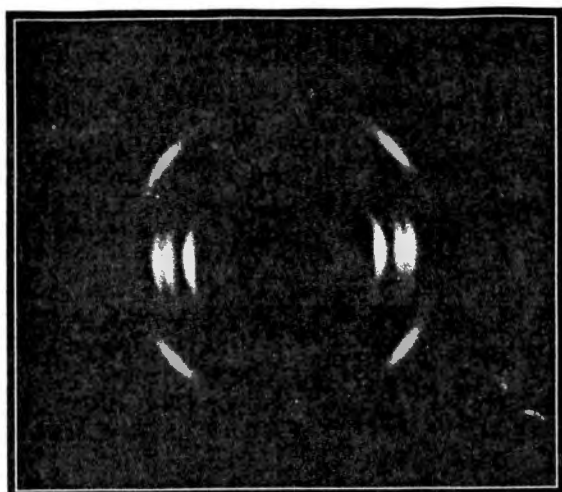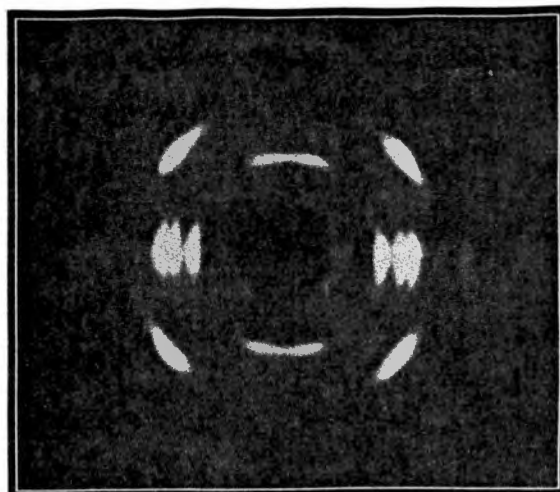
As-spun 1

As-spun 2

As-spun 3

Drawn 1

Drawn 2

Drawn 3

Figure 4.3 WAXD Patterns of Staple Fibers

4.1.2 Web Properties

Tensile strength values of the webs from different fibers bonded over a wide range of bonding temperature are shown in Figure 4.4. It was observed that web strength decreased with increase in fiber molecular orientation and crystallinity. Fibers with relatively less developed morphology yielded stronger webs as compared to fibers with more developed morphology. Bechter et al. [3] and Wei et al. [4] have also studied the effect of fiber draw-ratio on polypropylene nonwoven fabric properties and reported that fibers with lower draw-ratio resulted in fabric with higher tensile strength. Fiber to web strength 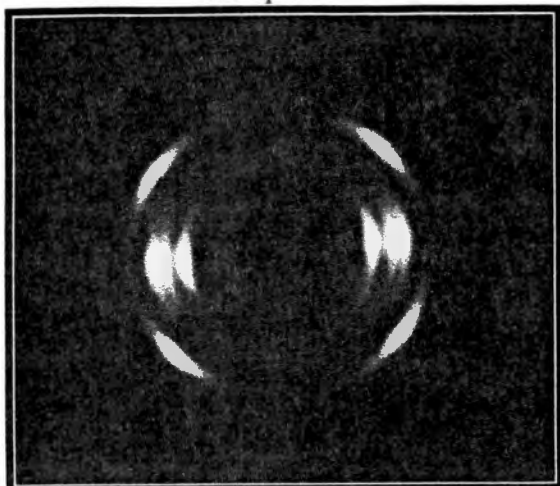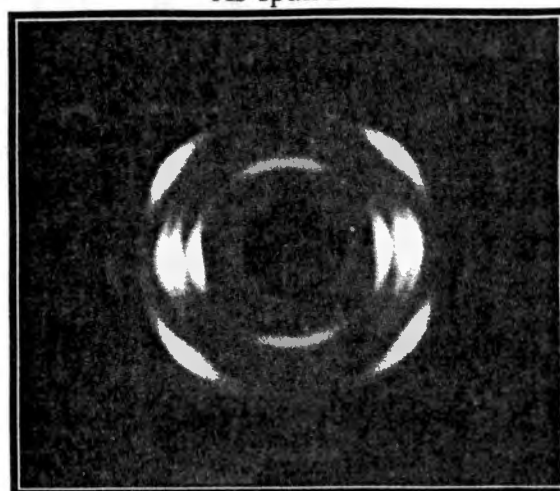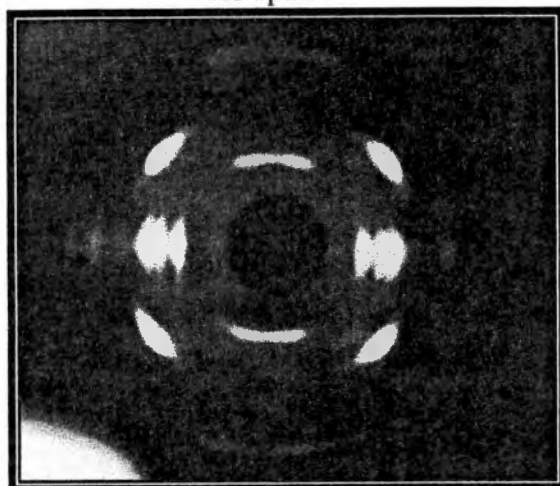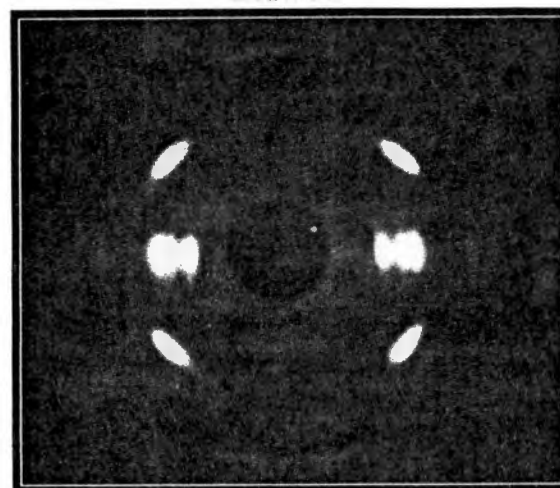realization for different fibers is shown in Figure 4.5. Fiber to web strength realization decreased sharply with increase in fiber molecular orientation and crystallinity. Web breaking-extension, initial modulus and toughness are shown in Figures 4.6, 4.7, and 4.8, respectively. Web breaking extension and toughness both exhibited a trend similar to tensile strength. However, initial modulus did not show any optimum and continued to increase with increase in bonding temperature. Higher strength, breaking extension, initial modulus, and toughness of the webs produced from the fibers having less molecular orientation and crystallinity may be partly attributed to higher breaking extension of the fibers. Higher breaking extension of the fibers leads to greater degree of load sharing between the fibers during the deformation of the web. Optimum bonding temperature for drawn fibers was found to be higher than that for as-spun fibers. Further, optimizing the bonding temperature did not help much in the case of highly drawn fibers, as can be seen from the web strength versus bonding temperature relationship. The optimum bonding temperature corresponded very well to the morphology of the fibers. Fibers with higher crystallinity and orientation required higher

46

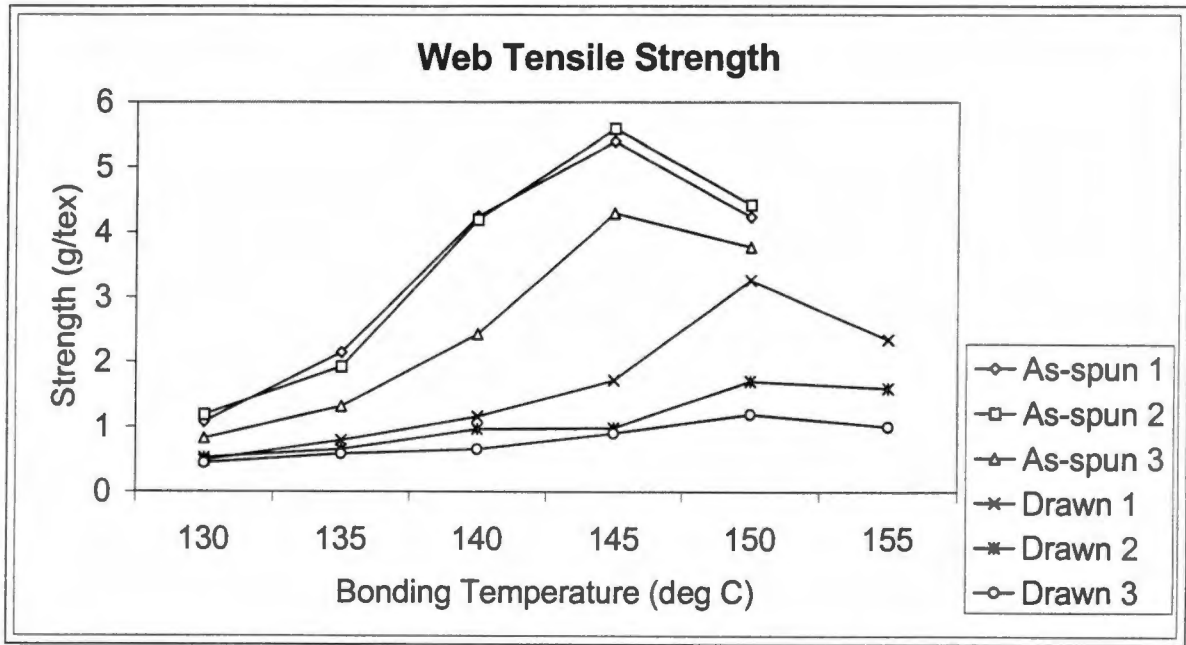**Figure 4.4 Web Tensile Strength (MD) vs Bonding Temperature for Staple Fibers**
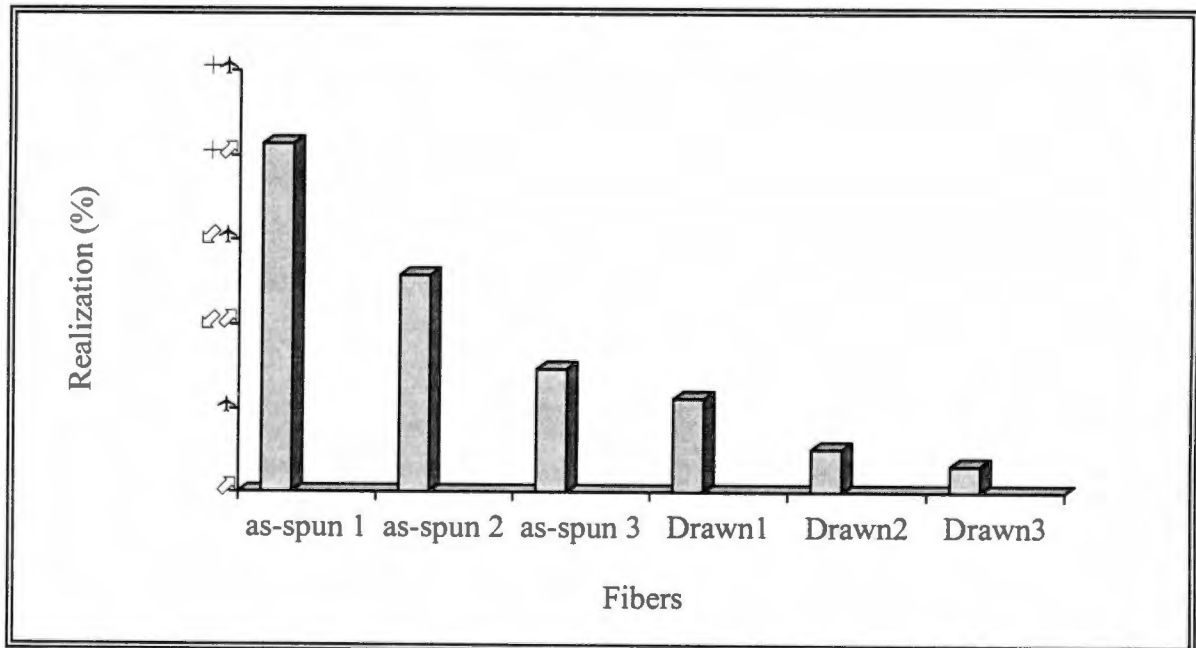
Figure 4.5 Fiber to Web Strength Realization for Staple Fibers
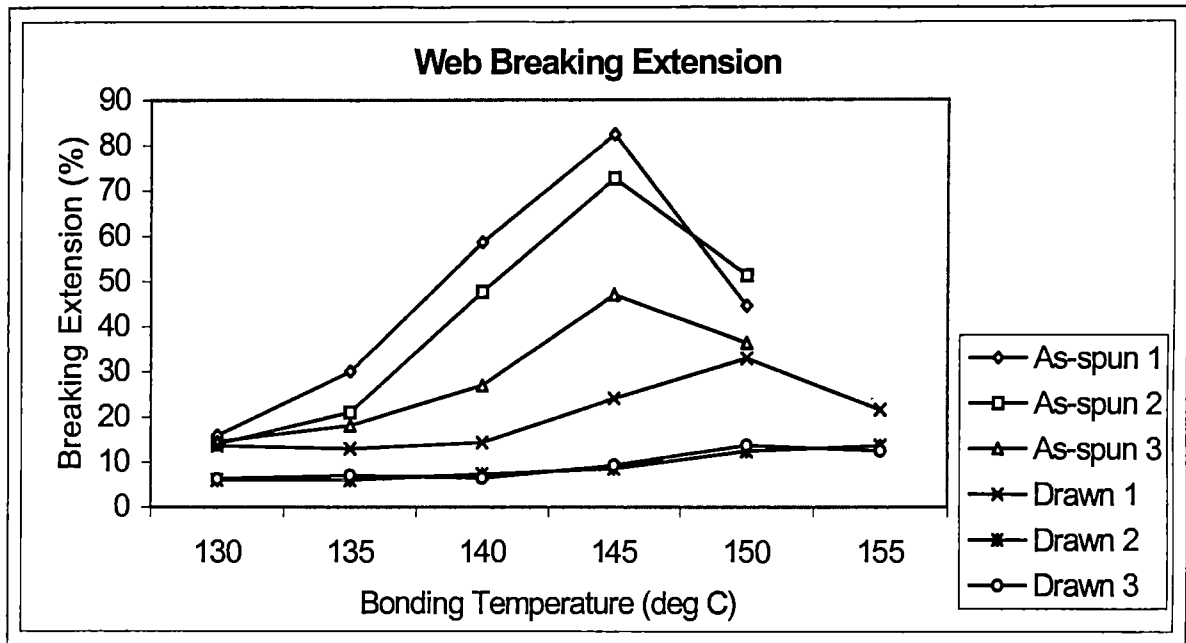
Figure 4.6 Web Breaking Extension vs Bonding Temperature for Staple Fibers
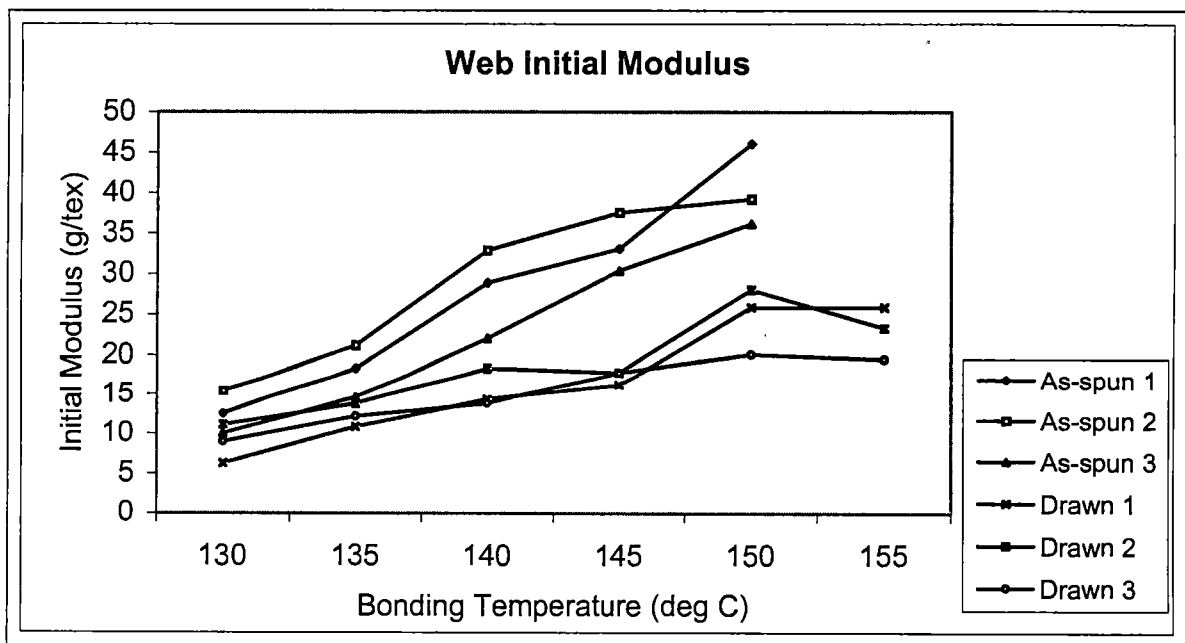
Figure 4.7 Web Initial Modulus vs Bonding Temperature for Staple Fibers

48
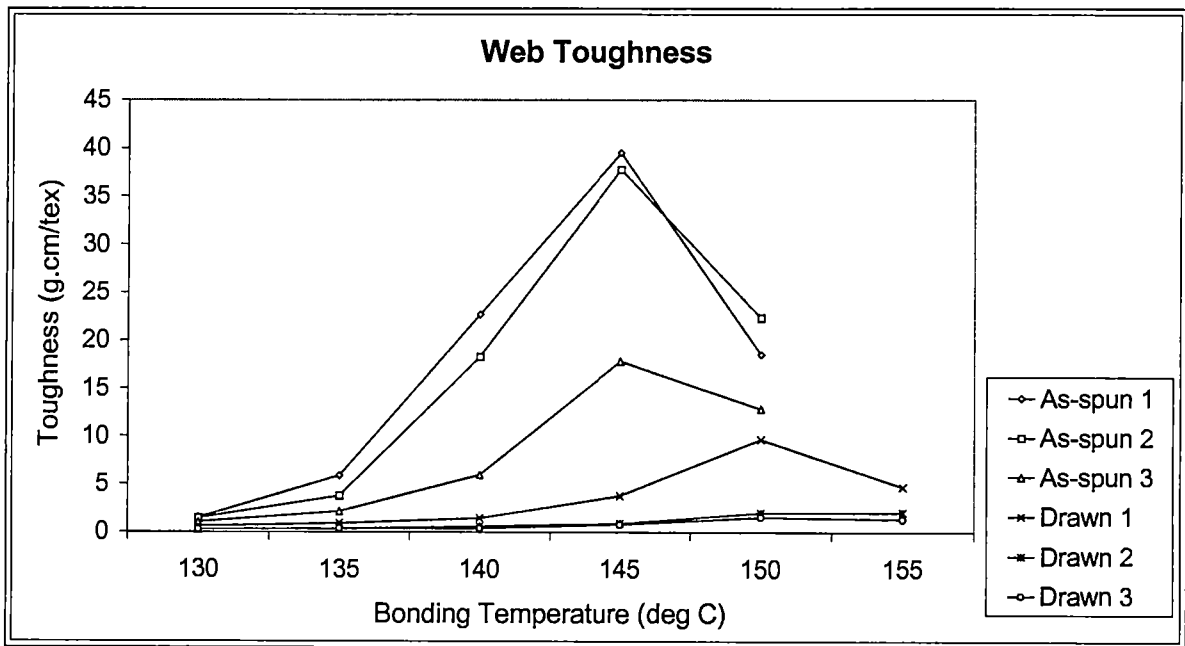
Figure 4.8 Web Toughness vs Bonding Temperature for Staple Fibers

bonding temperature. A good correlation was also observed between the bondability of the fibers and the TMA failure temperature of the fibers. The higher the TMA failure temperature, the higher the temperature required to bond the fibers well. A detailed analysis of the differences in bonding behavior of the fibers with different morphology is done in the next section.

4.1.3 Analysis and Discussion

Fracture mechanism of the webs was studied using an optical microscope and a scanning electron microscope (SEM). Optical micrographs of the bonds after the tensile test are shown in Figures 4.9 and 4.10, at optimum bonding temperatures, for as-spun and drawn fibers, respectively. As can be seen from the figures, bonds did not rupture during web failure in the case of webs produced from as-spun fibers, for bonding temperature at and above the optimum. Whereas in the case of drawn fibers, web failure involved rupture of the bonds at all the bonding temperatures studied. It was observed that bonds were very weak and brittle in the case of drawn fibers. It is further evident from the image of "elongated" bond in Figure 4.9 that bonds were very ductile and strong in the case of as-spun fibers. Disintegration of the bonds during web failure in the case of drawn fibers is shown in Figures 4.11 and 4.12. Fibers are pulled out from the bond one by one during disintegration. A similar kind of disintegration of the bonds occurred in the case of as-spun fibers at low bonding temperatures. In the case of as-spun fibers, drop in web strength above optimum bonding temperature may be attributed to very severe thermomechanical damage to the fibers in bond vicinity at higher temperatures.

ELONGATED BOND IN THE WEBS FROM AS-SPUN FIBERS AT FRACTURE POINT (bonding temp. 145 °C)
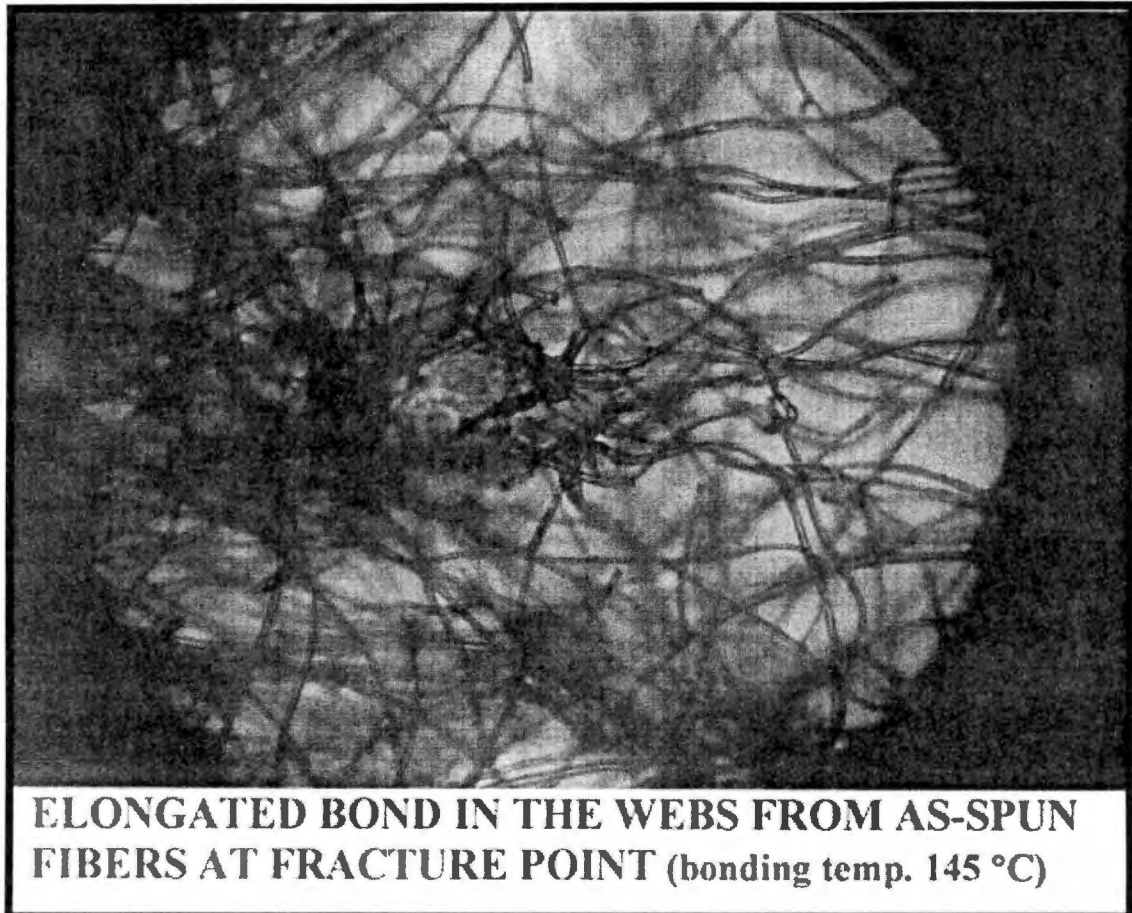
Figure 4.9 Optical Micrograph of a Bond after the Tensile Test for As-spun fibers

BOND RUPTURE IN THE WEBS FROM DRAWN FIBERS
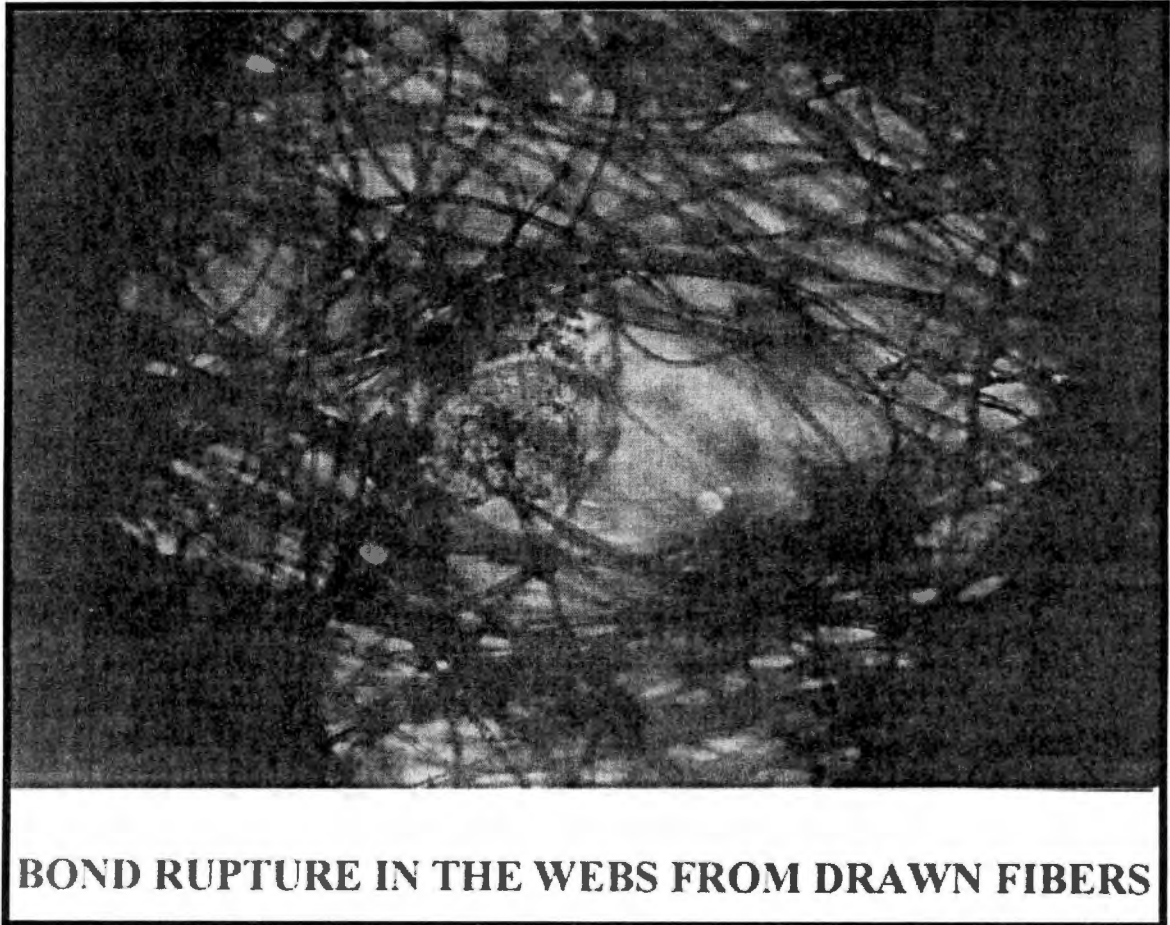
Figure 4.10 Optical Micrograph of a Bond after the Tensile Test for Drawn fibers

Figure 4.11 SEM Image Showing Disintegration of Bond (Intermediate Stage)

Figure 4.12 SEM Image Showing Disintegration of Bond (Final Stage)

Figures 4.13 and 4.14 show SEM images of bond point from untested webs for As-spun 1 and Drawn 1 fibers, respectively. It is evident from the figures that bond is not well formed and there is "less polymer flow" and "fibrillation of the fibers" in the bonded regions of the web in the case of drawn fibers. Insufficient polymer-flow, and fibrillation of the fibers appear to be the main factors responsible for weak and brittle nature of the bonds in the case of drawn fibers. No fibrillation was observed in the case of as-spun fibers. Fibrillation of the fibers is further clear from SEM images in Figures 4.15, 4.16 & 4.17. In case of drawn fibers, polymer flow could be improved with increase in bonding temperature, as can be seen in Figures 4.18 and 4.19. However, web failure occurred due to rupture of the bonds even at higher bonding temperatures. This is a clear indication of the brittleness of the bond for drawn fibers. In the case of as-spun fibers, bonds were ductile as indicated before due to good flow of polymer during bonding. The inter-fiber film formation due to polymer flow increases the energy required to cause breakage, thus increasing the strength.

A single-bond strip tensile test was done in order to estimate the bond strength and the degree of load sharing between the fibers. The results of this test are shown in Table 4.4. In this test also, no failure of bond was observed in the case of as-spun fibers. Whereas, in the case of drawn fibers, bond failure was observed at breaking loads much less than that in the case of as-spun fibers. Therefore, it may be concluded that bonds were much stronger in case of as-spun fibers as compared to drawn fibers. The bonds became more brittle and weak with increase in draw ratio of the fibers. Difference in breaking loads between as-spun fibers, as there was no failure of bonds, was attributed to difference in the degree of load sharing between the fibers. The degree of load sharing

54
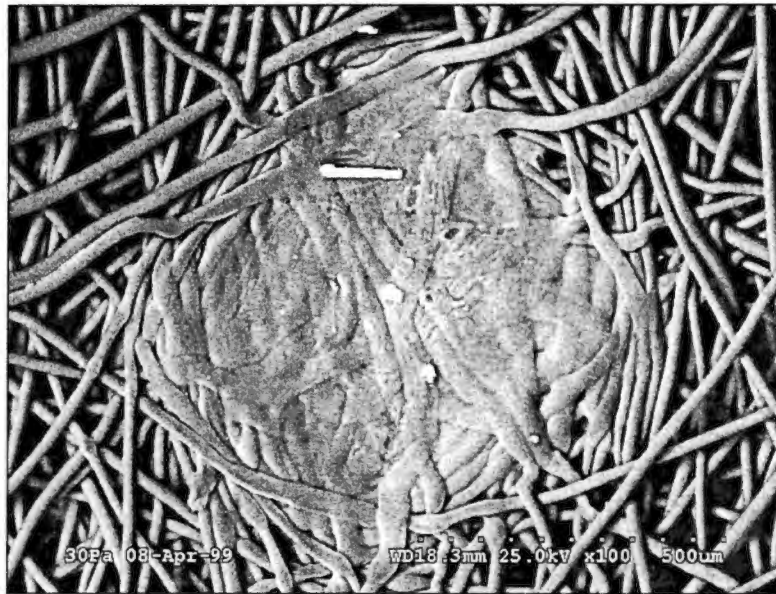
Figure 4.13 SEM Image of a Bond for As-spun 1 Fibers (145 °C)
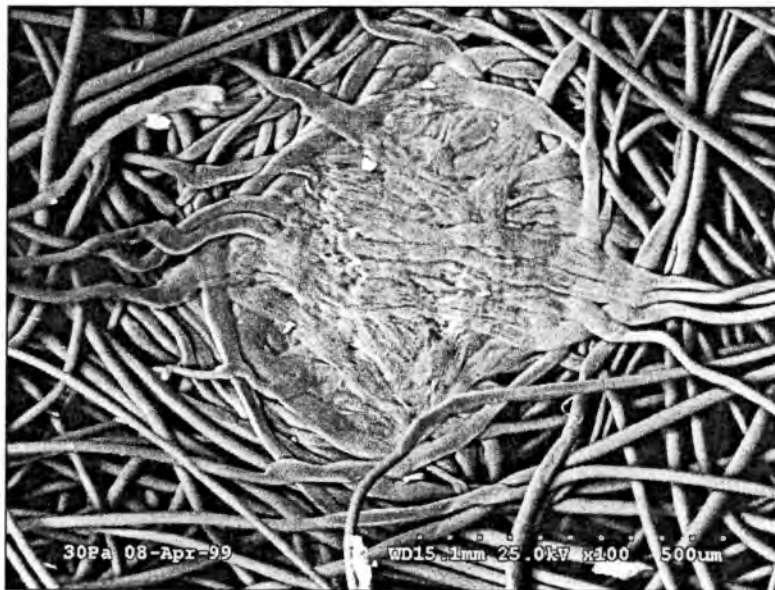
Figure 4.14 SEM Image of a Bond for Drawn 1 Fibers (145 °C)

55

Figure 4.15 SEM Image of a Bond for As-spun 1 Fibers at Higher Magnification (x500)
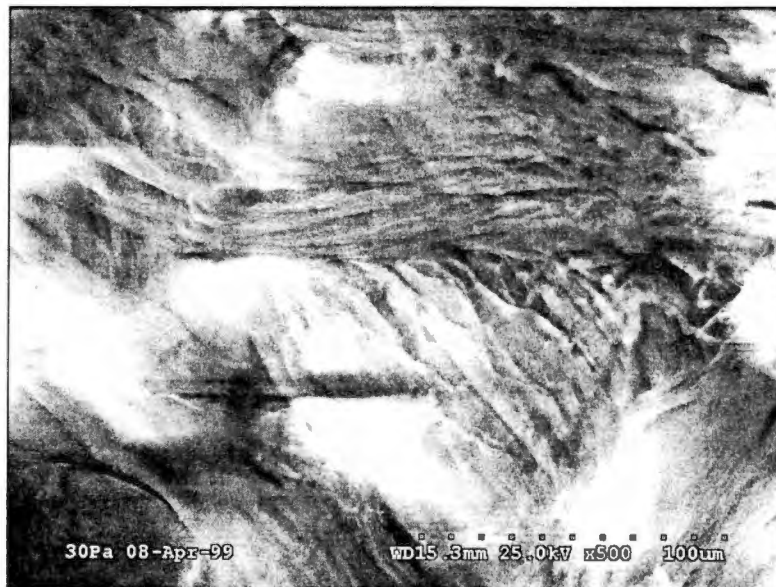
Figure 4.16 SEM Image of a Bond for Drawn 1 Fibers at Higher Magnification (x500)
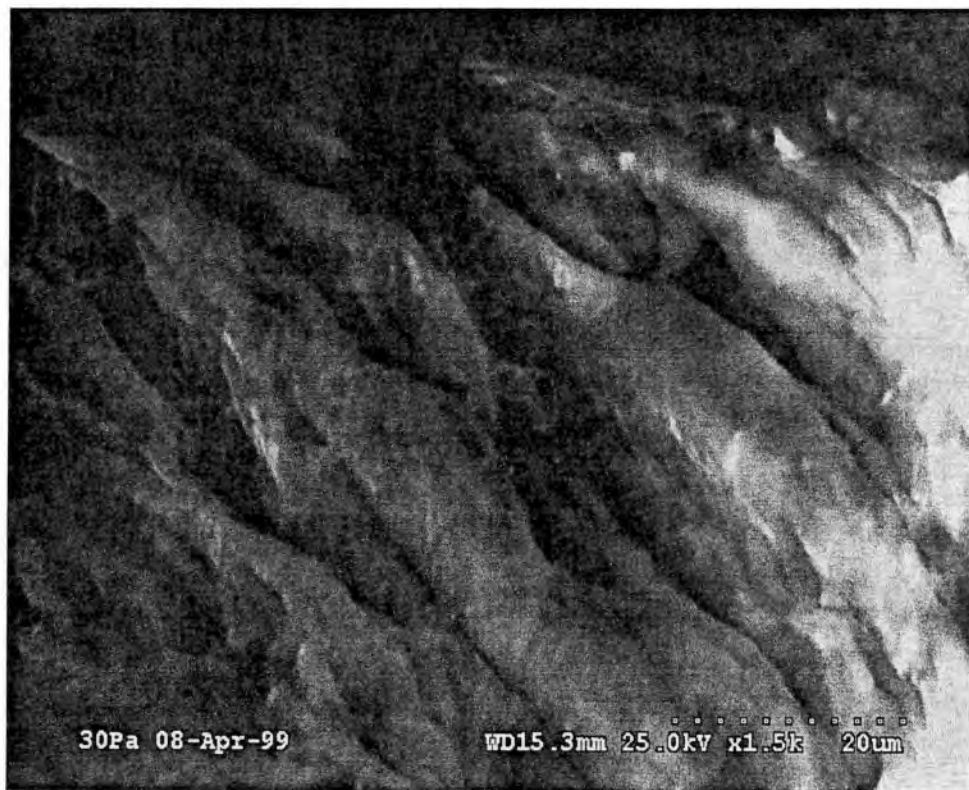
Figure 4.17 SEM Image of a Bond for Drawn 1 Fibers at Higher Magnification (x1500)
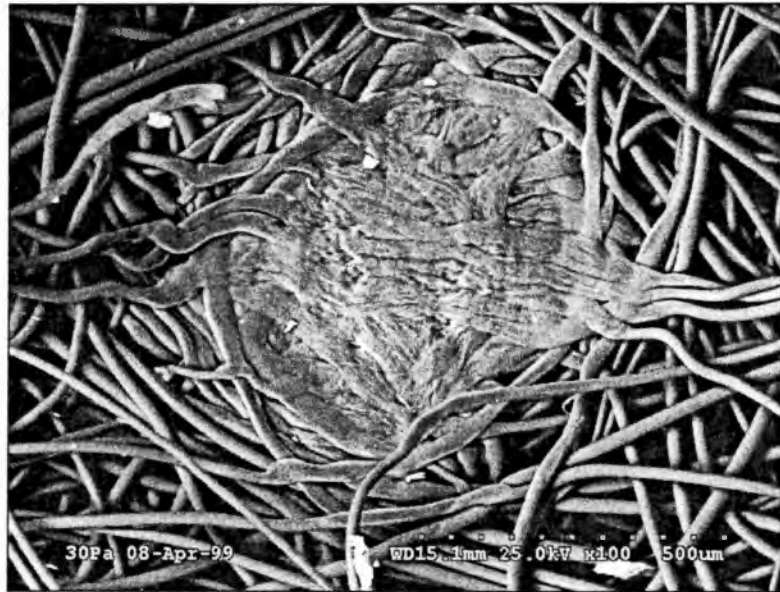
Figure 4.18 SEM Image of a Bond for Drawn 1 Fibers at 145 °C Bonding Temperature
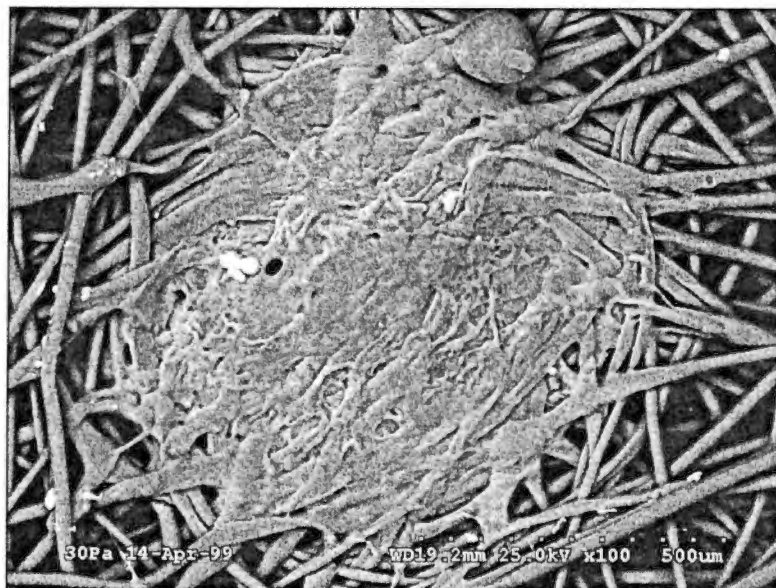
Figure 4.19 SEM Image of a Bond for Drawn 1 Fibers at 155 °C Bonding Temperature

Table 4.4 Results of Single-Bond Strip Tensile Test

SAMPLE ID	BREAKING LOAD (G)	BREAKING EXTENSION (%)	NATURE OF BOND FAILURE
As-spun 1	260	16.9	No failure
As-spun 2	212	17.9	No failure
As-spun 3	154	11.7	No failure
Drawn 1	96	7.3	Semi-ductile
Drawn 2	74	5.1	Brittle
Drawn 3	73	4.8	Very brittle

between the fibers was directly related to breaking extension of the fibers. Higher the breaking extension, higher the degree of load sharing.

Web properties may be greatly affected by the orientation distribution of the fibers in the web. Orientation ratio, the ratio of the number of the fibers in machine direction to that in cross direction of the web, is reported in Table 4.5, for two bonding temperatures. The small differences in orientation ratio were observed between as-spun and drawn fibers, but such small differences should not have been responsible for the drastic differences observed in web properties between as-spun and drawn fibers.

4.2 Spunbond Studies

4.2.1 Fiber Properties

The properties of spunbond fibers for all the three sets are listed in Tables 4.6, 4.7 & 4.8. DSC scans are shown in Figure 4.20. Thermomechanical (TMA) responses of the fibers are shown in Figure 4.21. WAXD photographs are shown in Figure 4.22. The results show that three sets differed significantly in terms of their molecular-orientation, crystallinity, crystallite size and other morphological aspects. Fiber diameter was within the desired range for all the three sets. As in the case of staple fiber studies, fiber diameter was intentionally kept the same so that the differences due to change in diameter could be minimized and the role of fiber micro-morphology in thermal bonding could be analyzed. Set I fibers had the most developed morphology followed by Set II and Set III, respectively. The same was supported by TMA and tensile-test data. As can be seen from TMA failure temperature for different sets, Set I fibers had the highest thermo-mechanical stability followed by Set II and Set III, respectively. Diffused peaks

Table 4.5 Orientation Factor of Staple Fiber Webs (From Webpro)

SAMPLE ID	ORIENTATION RATIO OF THE WEBS	
	Bonding Temperature 130 °C	Bonding Temperature 145 °C
As-spun 1	2.1	2.2
As-spun 2	2.2	2.2
As-spun 3	1.8	1.9
Drawn 1	1.4	1.5
Drawn 2	1.6	1.5
Drawn 3	1.4	1.4

Table 4.6 Spunbond Fibers Morphological Parameters

SAMPLE ID	DIAMETER (μM)	BIREFRINGENCE ($X \times 10^{-3}$)	CRYSTALLINITY (%)	CRYSTAL SIZE (A°)
Set I	19.3	21.8	45.4	110
Set II	19.3	21.2	46.5	50
Set III	18.8	18.8	47.3	35

Table 4.7 Spunbond Fibers Thermomechanical Properties

SAMPLE ID	TMA SHRINKAGE (%)	TMA FAILURE TEMP. AT LOW TENSION (°C)	TMA FAILURE TEMP. AT HIGH TENSION (°C)
Set I	10.5	159	109
Set II	8.5	154	89
Set III	6.0	153	66

Table 4.8 Spunbond Fibers Tensile Properties

SAMPLE ID	TENACITY (GPD)	BREAKING EXTENSION (%)
Set I	3.1	300
Set II	2.7	280
Set III	2.4	225
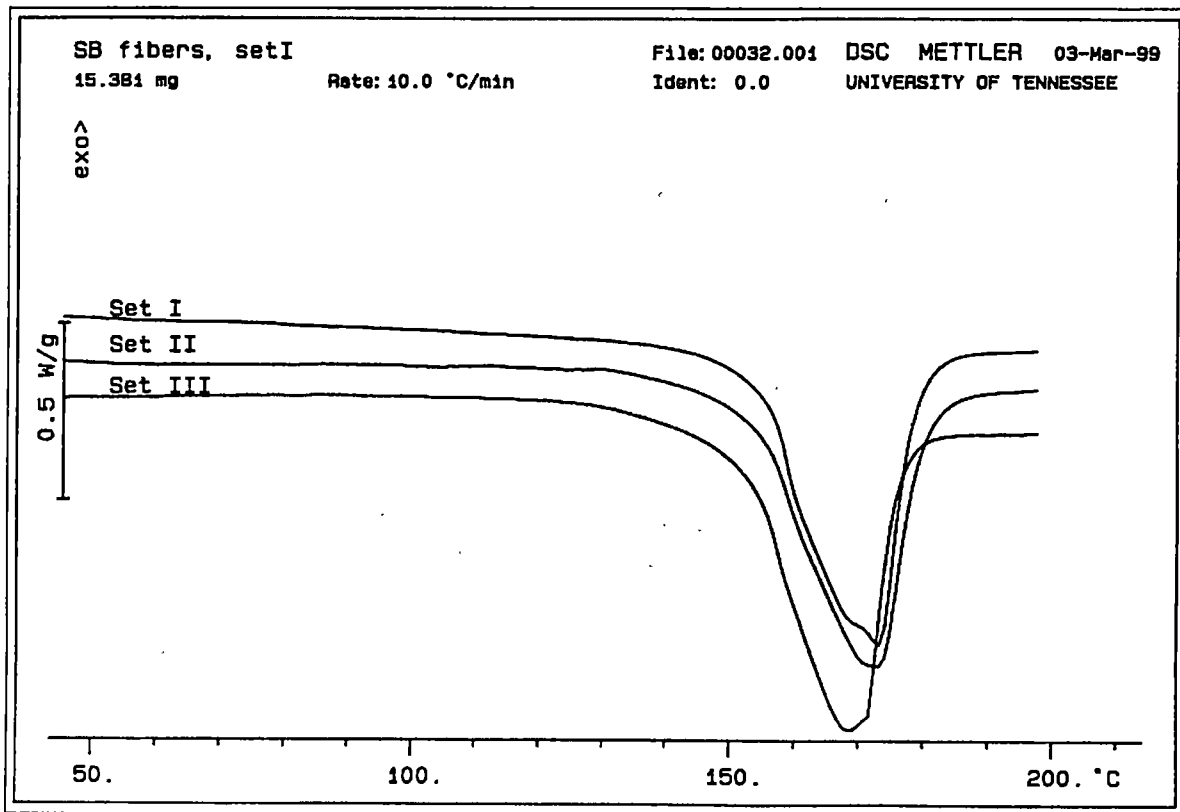
Figure 4.20 DSC Scans of Spunbond Fibers

SB fibers, setI, 0.005N/7   File:00013.001 TMA METTLER 17-Feb-99
10.000 mm   Rate: 10.0 °C/min Ident: 0.0   UNIVERSITY OF TENNESSEE

Set I

Set II

Set III

μm

2000.

50.   100.   150.   °C
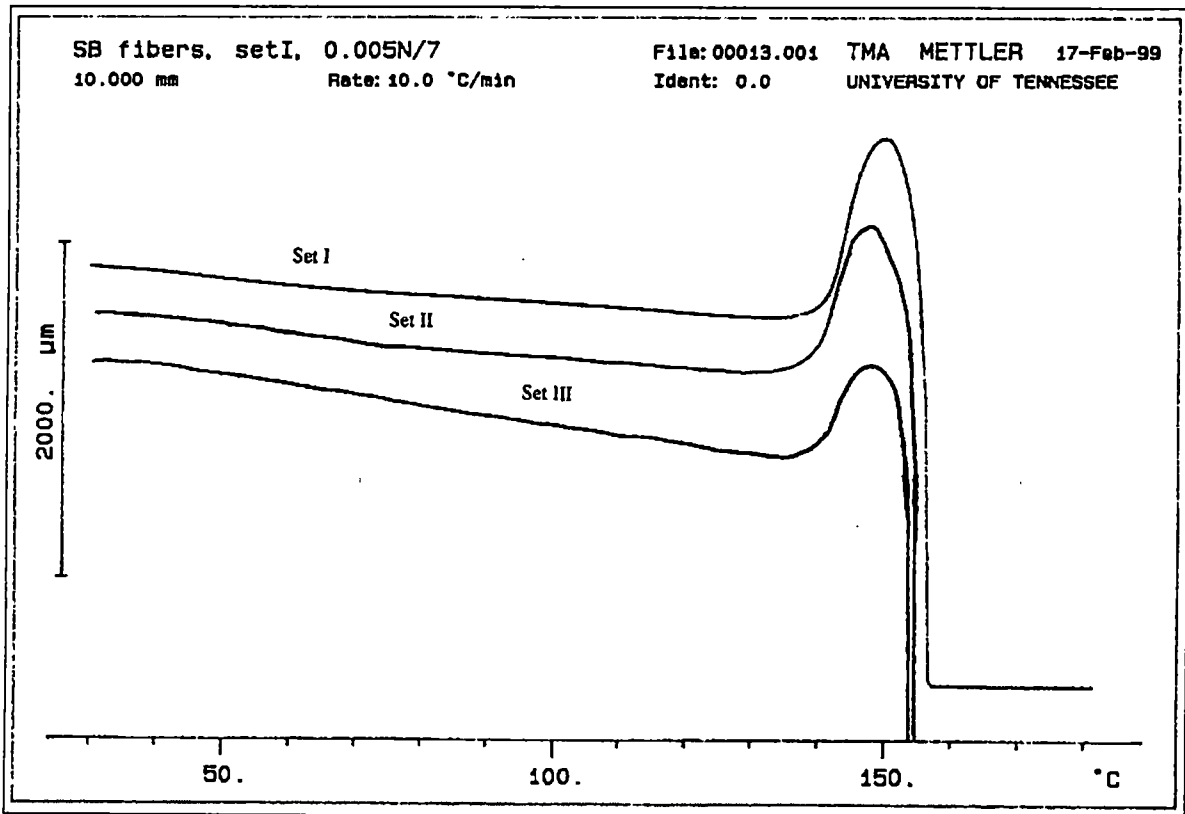
(a)

Figure 4.21 Thermo-mechanical Responses of Spunbond Fibers at Low (a) and High
(b) Tension

64

SB fibers, setI, 0.05N/7   File: 00019.001   TMA   METTLER   18-Feb-99
10.000 mm   Rate: 10.0 °C/min   Ident: 0.0   UNIVERSITY OF TENNESSEE

5000. µm

Set III   Set II   Set I

50.   100.   150.   °C
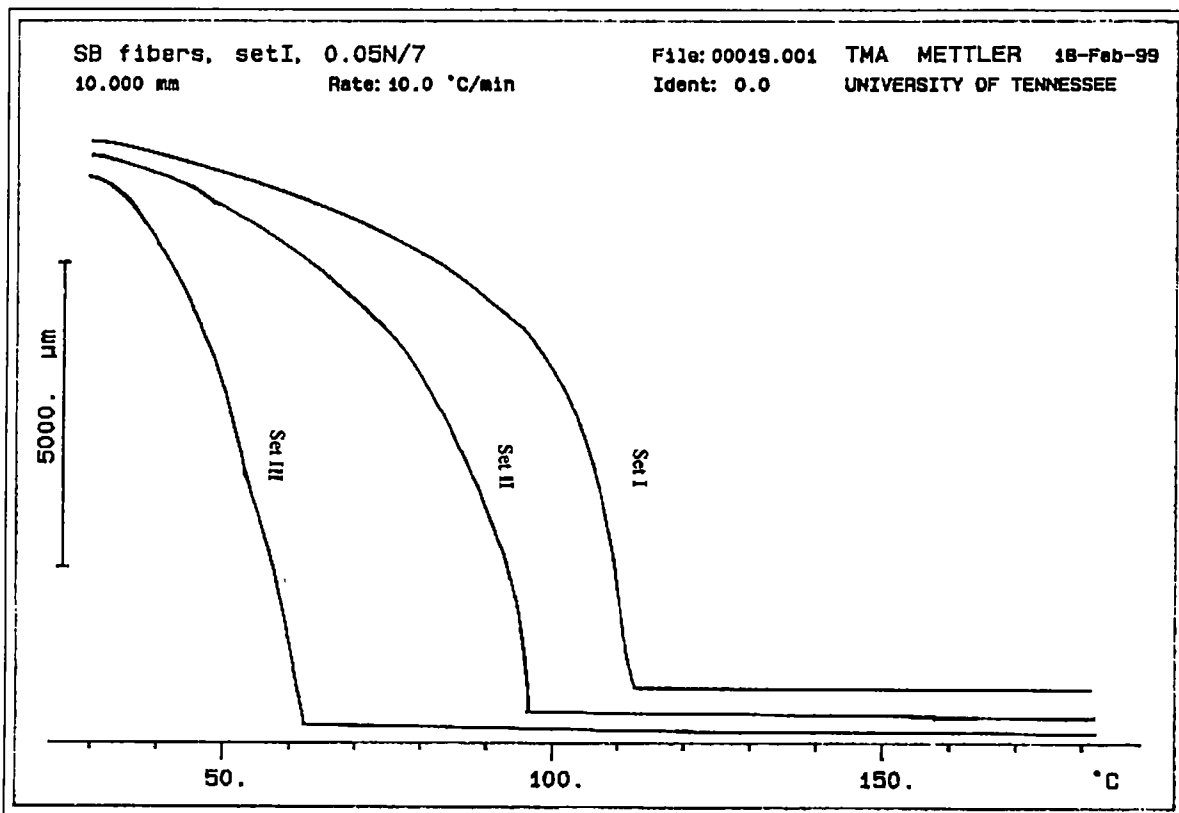
(b)

Figure 4.21 (Continued)

65
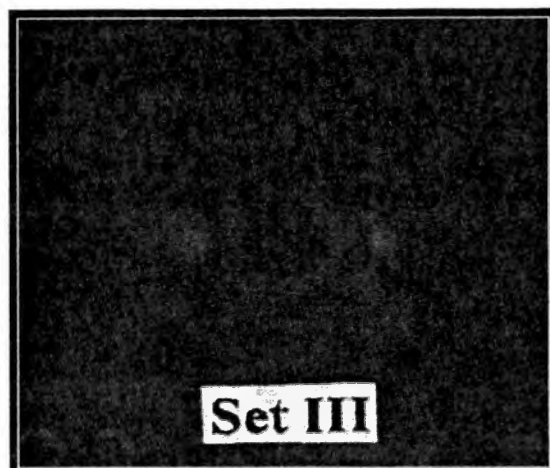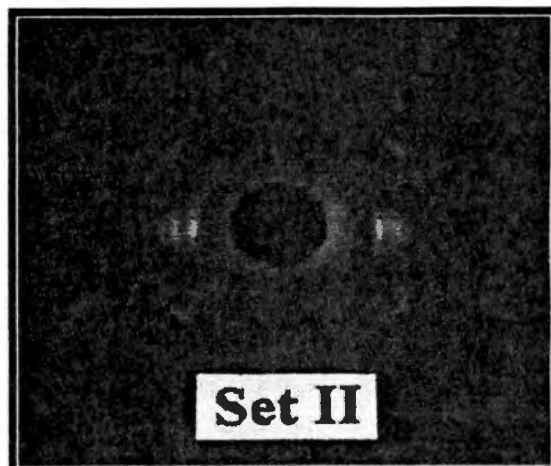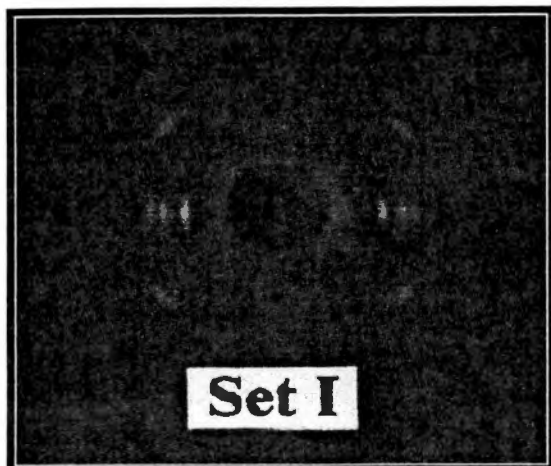
Figure 4.22 WAXD Patterns of Spunbond Fibers

in WAXD pattern of Set III fibers indicate the significant presence of "smectic" phase in Set III fibers. Formation of smectic phase is favored at higher melt temperature [61], as was the case for Set III. Fiber birefringence and breaking extension of spunbond fibers did not go hand in hand. Presence of smectic phase may be responsible for lower breaking extension of Set III fibers, in spite of their lower birefringence.

4.2.2 Web Properties

Differences in web properties for different sets were small in the case of spunbond webs owing to small differences in their fiber properties. Tensile strength of the spunbond webs from different sets of the fibers bonded over a wide range of bonding temperature is shown in Figure 4.23. Maximum web strength achieved for Set III fibers was less than that for Set I & II. Lower strength of Set III webs may be attributed to relatively lower fiber tenacity as well as breaking extension. However, optimum bonding temperature was the lowest for Set III fibers followed by Set II and Set I, respectively. Better bondability of Set III fibers may be assigned to their smaller crystal size, paracrystalline structure and less molecular orientation, which provide better polymer flow at lower temperatures. A good correlation was observed between the TMA failure temperature and the optimum bonding temperature of the fibers as seen with staple fiber studies. Fibers with lower TMA failure temperature, such as Set III, had lower optimum bonding temperature than the fibers with higher TMA failure temperature, such as Set I. A similar kind of correlation between the TMA failure temperature and the bonding temperature has been reported by Zhang et al. [48]. Improved bondability of the fibers
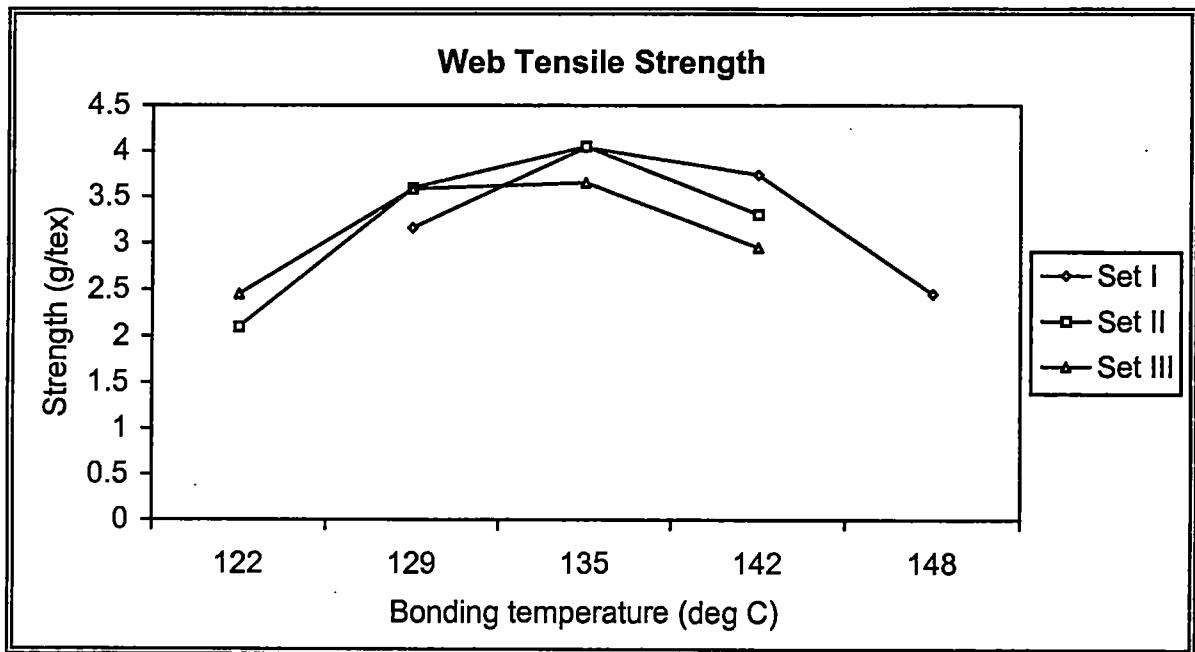
Figure 4.23 Tensile Strength vs Bonding Temperature for Spunbond Webs

from Set I to Set III could also be seen in terms of increase in fiber to web strength realization from Set I to Set III, as shown in Figure 4.24. Web breaking-extension, initial modulus, toughness and bursting strength are shown in Figures 4.25, 4.26, 4.27 and 4.28, respectively. Higher tensile strength, breaking extension and toughness of Set III webs at lower bonding temperatures may again be attributed to better bondability of Set III fibers. However, as can be seen from Figures 4.23, 4.25, & 4.27, the trend in web properties for different sets reversed from lower to higher temperature. Two competing factors in this case may be speculated to be the bondability and the mechanical properties of the fibers. At lower bonding temperatures, bondability of the fibers seemed to dominate the web properties, and at higher bonding temperatures, mechanical properties of the fibers were dominant. Web initial modulus increased with increase in bonding temperature. Web initial modulus was the highest for Set I fibers due to their higher molecular orientation. Further analysis of bonding behavior of different spunbond fibers is reported in the next section.

4.2.3 Analysis and Discussion

Bonding behavior of spunbond webs was also studied using the scanning electron microscope. Figure 4.29 shows SEM images of bond points from untested webs for all three sets. As can be seen, the bond was well formed with sufficient polymer flow, for all the fibers at 135 °C. At the same time, fiber integrity was not completely lost at optimum bonding temperatures. In the case of spunbond webs, for bonding temperatures at and above optimum, failure occurred in bond vicinity as shown in Figure 4.30. In general,
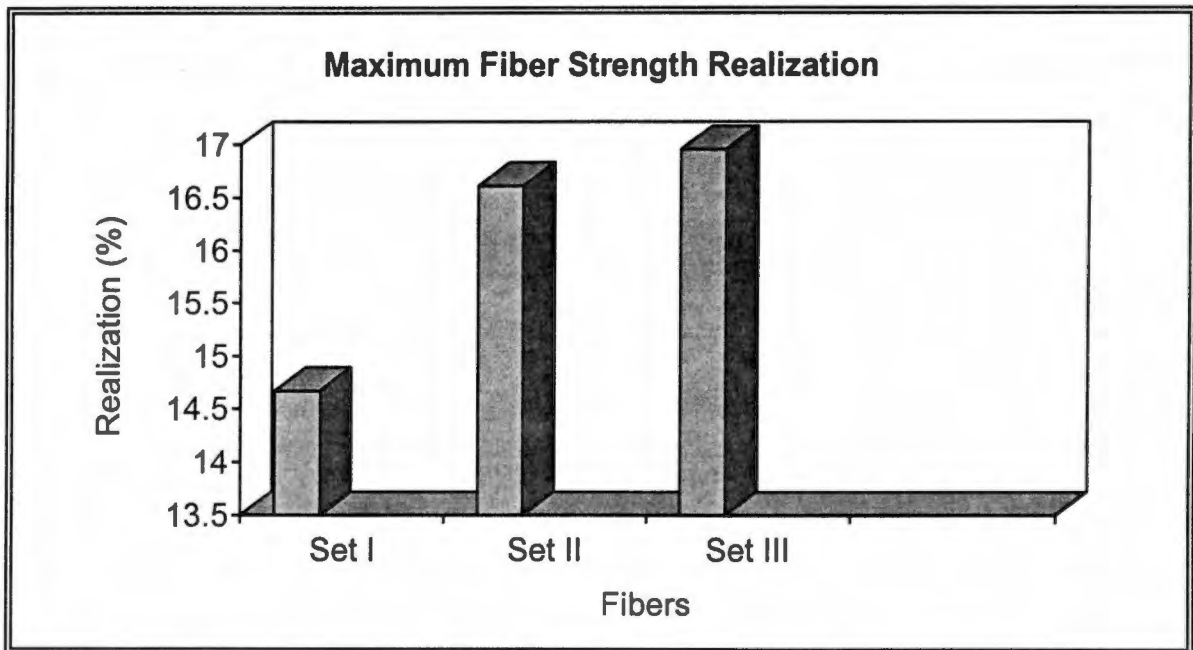
Figure 4.24 Maximum Fiber Strength Realization for Spunbond Fibers
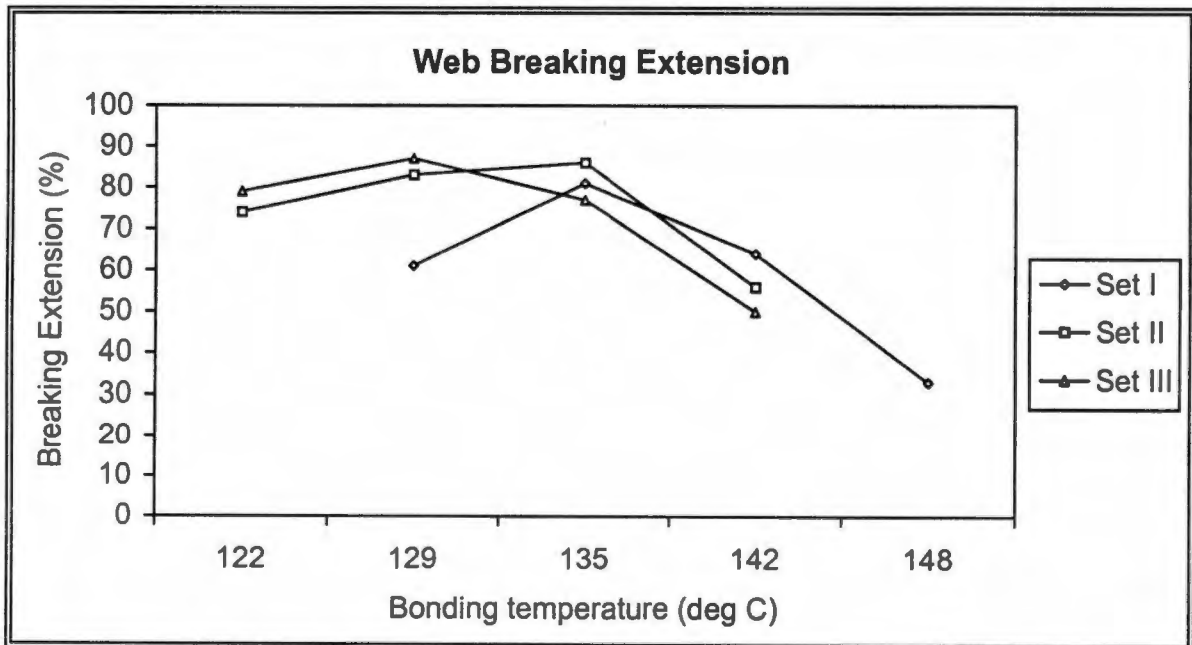
Figure 4.25 Breaking Extension vs Bonding Temperature for Spunbond Webs
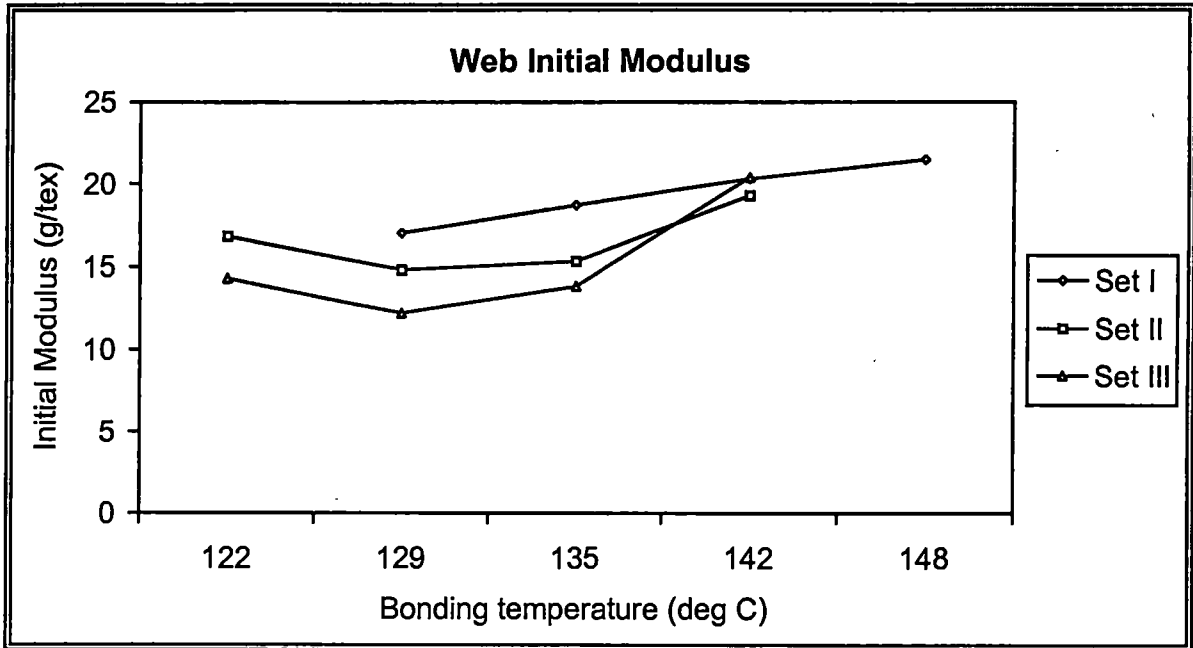
Figure 4.26 Initial Modulus vs Bonding Temperature for Spunbond Webs
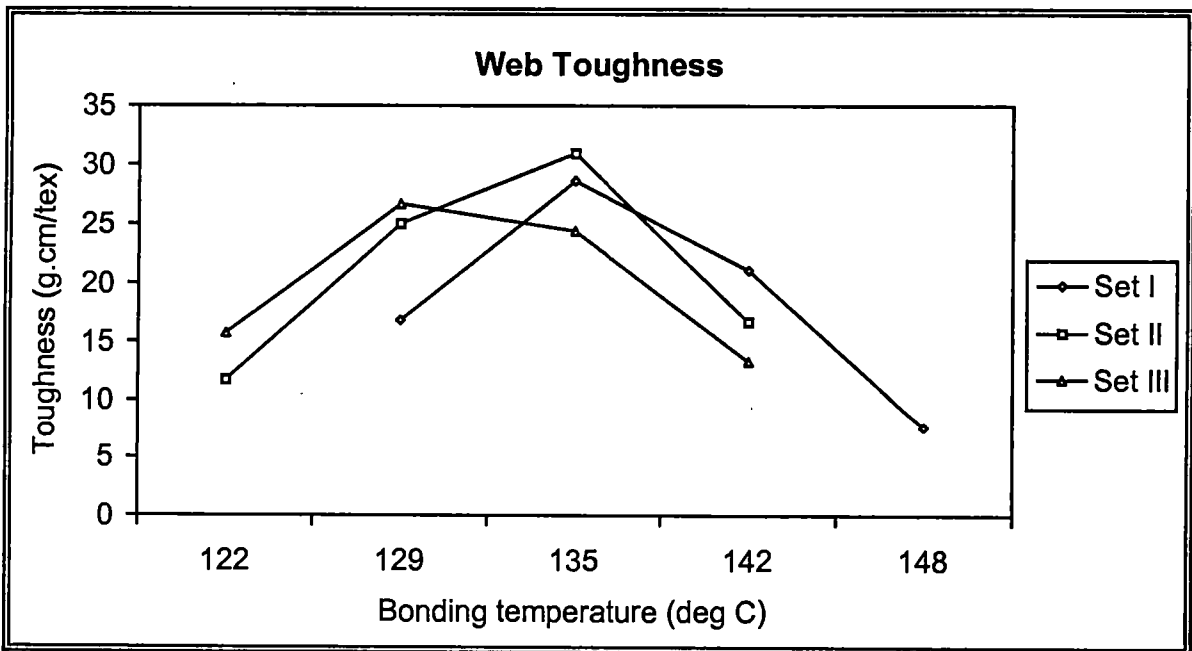
Figure 4.27 Toughness vs Bonding Temperature for Spunbond Webs

71
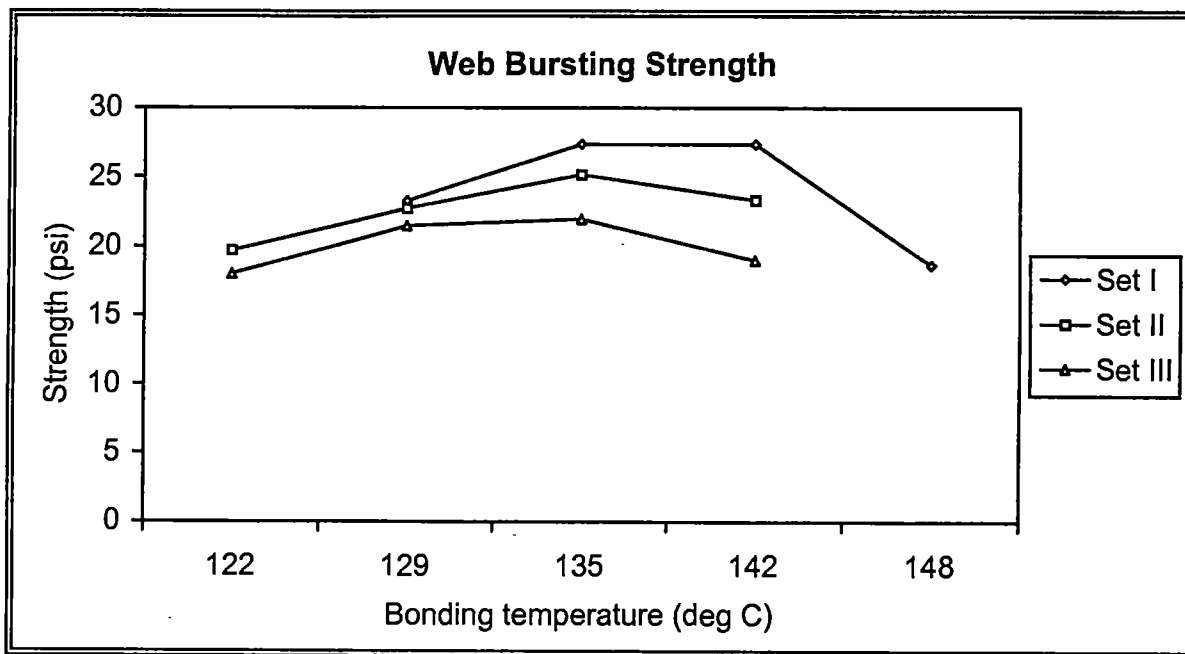
Figure 4.28 Bursting Strength vs Bonding Temperature for Spunbond Webs
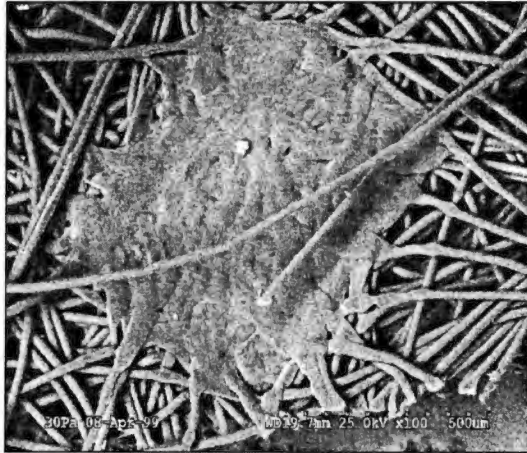
Set I
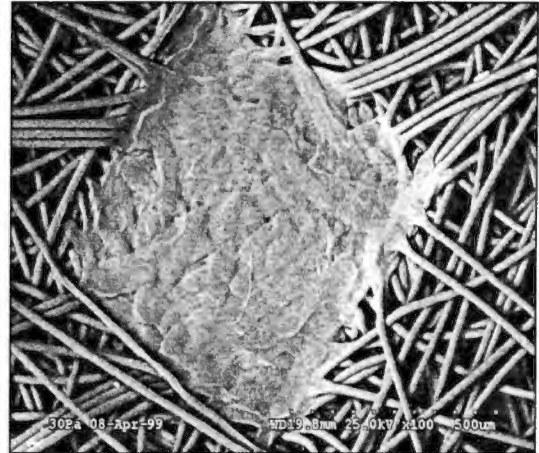
Set II
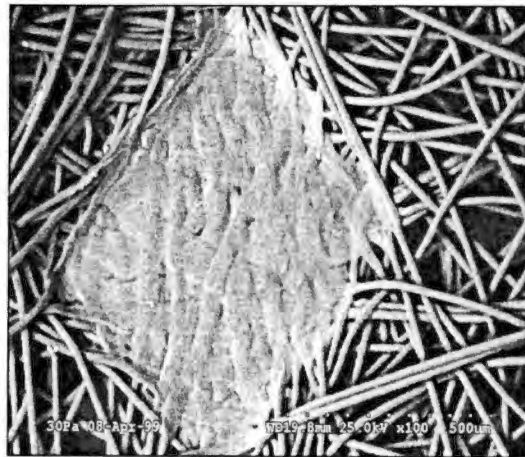
Set III

Figure 4.29 SEM Images of Bonds From Spunbond Webs (135 °C)
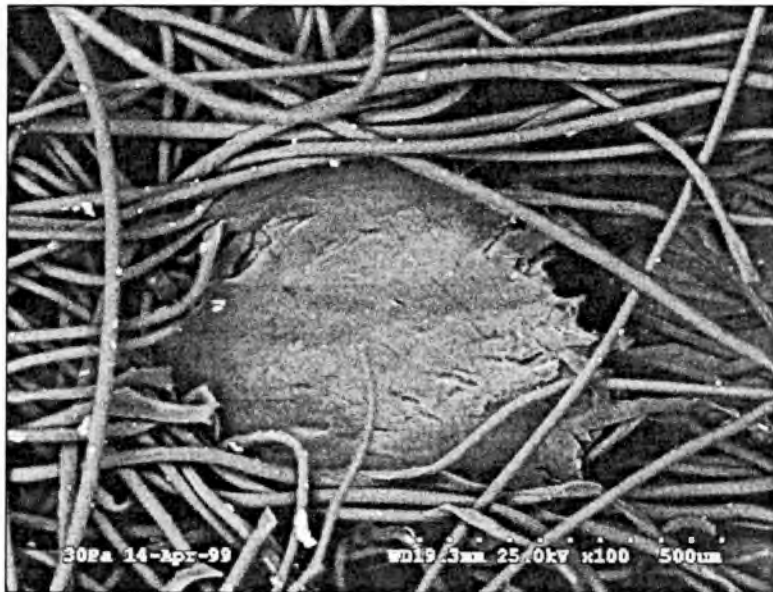
Figure 4.30 SEM Image of a Spunbond Web Showing Failure in Bond Vicinity

bonding behavior of spunbond fibers was similar to that of as-spun staple fibers. However, maximum web strength achieved was lower in the case of spunbond webs as compared to as-spun staple fiber webs. The main factor responsible for such differences seem to be the difference in polymer MFR used for two studies. Other small factors may be differences in bonding speed and fiber distribution in the webs.

Single bond strip tensile test for the webs bonded at 135 °C showed no rupture of bond in either case. Breaking strength was 183, 165 and 171 grams for Set I, Set II, and Set III, respectively. Again, such small differences were due to small differences in spunbond fibers. Malkan et al. [14] have reported the rupture of bonds in spunbond webs at higher bonding temperatures. Such differences in observations may be most probably due to differences in the range of bonding temperature covered in the studies. In our studies, no rupture of bonds was observed at temperatures just above the optimum bonding temperature. However, rupture of the bonds as reported by Malkan et al. may happen at very high bonding temperatures.

4.3 Morphological Changes During Thermal Bonding

Morphological changes in the fibers were studied at a medium (close to optimum for all) bonding temperature, which was 145 °C in the case of staple fiber studies, and 135 °C in the case of spunbond studies. Significant changes in fiber structure were observed in both the cases. The effects were less prominent in the case of spunbond studies as compared to staple fiber studies due to much lower residence time at the bonding temperature for the spunbond studies. Table 4.9 shows the change in molecular orientation of the fibers during the thermal bonding process. Birefringence of the fibers

75

Table 4.9 Change in Molecular Orientation during Thermal Bonding

SAMPLE ID	BIREFRINGENCE OF VIRGIN FIBERS $(X \times 10^{-3})$	BIREFRINGENCE IN UNBONDED REGION $(X \times 10^{-3})$	BONDED REGION[*] (% SHRINKAGE)
As-spun 1	19.0	23.3	1.9
As-spun 2	20.4	23.4	4.5
As-spun 3	17.8	25.0	3.7
Drawn 1	23.8	26.6	10.6
Drawn 2	29.4	29.6	16.8
Drawn 3	31.4	30.6	19.4
Set I	21.8	21.6	22.6
Set II	21.2	22.3	18.3
Set III	18.8	22.4	24.0

* In bonded regions, molecular orientation was estimated in terms of change in bond-dimensions when heated up to 160 °C. For details, please see Chapter 3.

increased as a result of annealing under constrained length during calendering. It was also observed that birefringence of the fiber did not change significantly from one point to another between two bond points, except a transitional zone of ≈50 μm in bond vicinity. Increase in birefringence was more for the fibers with comparatively less developed morphology. Since it was almost impossible to measure the birefringence of bonded regions, retained molecular orientation in bonded regions was estimated in terms of change in bond dimensions when bonds were heated up to 160 °C just below the melting point. Retained molecular orientation was higher for the fibers having higher molecular orientation in the beginning. Relatively higher level of bond shrinkage in spunbond may be attributed to low residence time, which led to less relaxation of the molecules in the bonded regions during the bonding process.

Table 4.10 shows change in crystallinity of the fibers during thermal bonding. A significant increase in crystallinity was observed from virgin fibers to bonded as well as unbonded regions of the web, in the case of staple fiber studies. Such a significant increase may be due to much higher residence time in the case of staple fiber studies, which allowed significant recrystallization to occur. No significant changes in crystallinity were observed in spunbonding. It was felt that crystallinity changes in spunbond studies may be very marginal and, therefore, crystallinity changes were also studied using density gradient column. The results from density gradient column are given in Table 4.11. Crystal size increased during thermal bonding in both staple fiber as well as spunbond studies, as shown in Table 4.12. Here it needs to be noted that crystal size data for the smectic phase are only good approximations. Increase in crystal size was even more significant for spunbond fibers. Crystals in the case of spunbond fibers grew

Table 4.10 Change in % Crystallinity (DSC) during Thermal Bonding

SAMPLE ID	CRYSTALLINITY OF VIRGIN FIBERS (%)	CRYSTALLINITY IN UNBONDED REGION (%)	CRYSTALLINITY IN BONDED REGION (%)
As-spun 1	36.7	41.9	50.1
As-spun 2	41.3	47.8	55.1
As-spun 3	45.0	48.3	58.8
Drawn 1	48.9	52.6	53.5
Drawn 2	53.7	54.2	54.3
Drawn 3	56.4	56.9	56.1
Set I	45.4	45.0	48.6
Set II	46.5	44.8	46.3
Set III	47.3	45.8	47.1

Table 4.11 Crystallinity of Spunbond Fibers and Webs Using Density Gradient Column

SAMPLE ID	CRYSTALLINITY OF FIBERS (%)	CRYSTALLINITY OF WEBS (%)
Set I	44.8	46.0
Set II	43.6	45.8
Set III	45.4	45.9

Table 4.12 Change in Crystal Size during Thermal Bonding

SAMPLE ID	CRYSTAL SIZE FOR VIRGIN FIBERS (A°)	CRYSTAL SIZE FOR UNBONDED REGION (A°)	CRYSTAL SIZE FOR BONDED REGION (A°)
As-spun 1	140	160	185
As-spun 2	185	215	245
As-spun 3	150	170	180
Drawn 1	140	165	190
Drawn 2	155	160	170
Drawn 3	135	145	160
Set I	110	145	170
Set II	50	130	145
Set III	35	90	160

bigger and fewer. Such a rearrangement of crystalline structure in spunbond fibers was also indicated by WAXD equatorial scans shown in the Figures 4.31, 4.32 & 4.33. Change in location and width of reflection peaks from virgin fibers to bonded and unbonded regions of the web suggested transformation of smectic phase to more stable and perfect monoclinic phase during thermal bonding process.

MFR of feed resin and webs was determined in order to compare the level of thermal degradation under different processing conditions in spunbonding. Results are shown in Table 4.13. Only a slight increase in the degree of thermal degradation was observed with increase in melt temperature from Set I to Set III. Thus, it is clear that differences in spunbonding conditions did not cause much variation in the polymer molecular weight and all the differences can be attributed to morphological differences.

4.4 Statistical Analysis

The results of statistical analyses are shown in Appendix I, II & III. There was enough evidence against the null hypothesis that the mean fiber tenacity was equal for Set I, Set II and Set III, and, the probability that it could happen by chance was 0.0003 (Appendix I). This means that differences in spunbond fibers, though small, are statistically significant. Statistically significant difference (Confidence level >95%) in web strength for different sets was observed only at higher bonding temperatures. However, significance level of differences in Set I, Set II and Set III could be improved if the test was done on tensile strength, breaking extension and toughness jointly as they showed the same trend with bonding temperature. The effect of bonding temperature on web strength was found to be very significant for all the three sets.

Table 4.13 Change in MFR From Resin to Spunbond Webs

MFR OF RESIN	MFR OF SET I WEBS	MFR OF SET II WEBS	MFR OF SET III WEBS
34	43	45	46
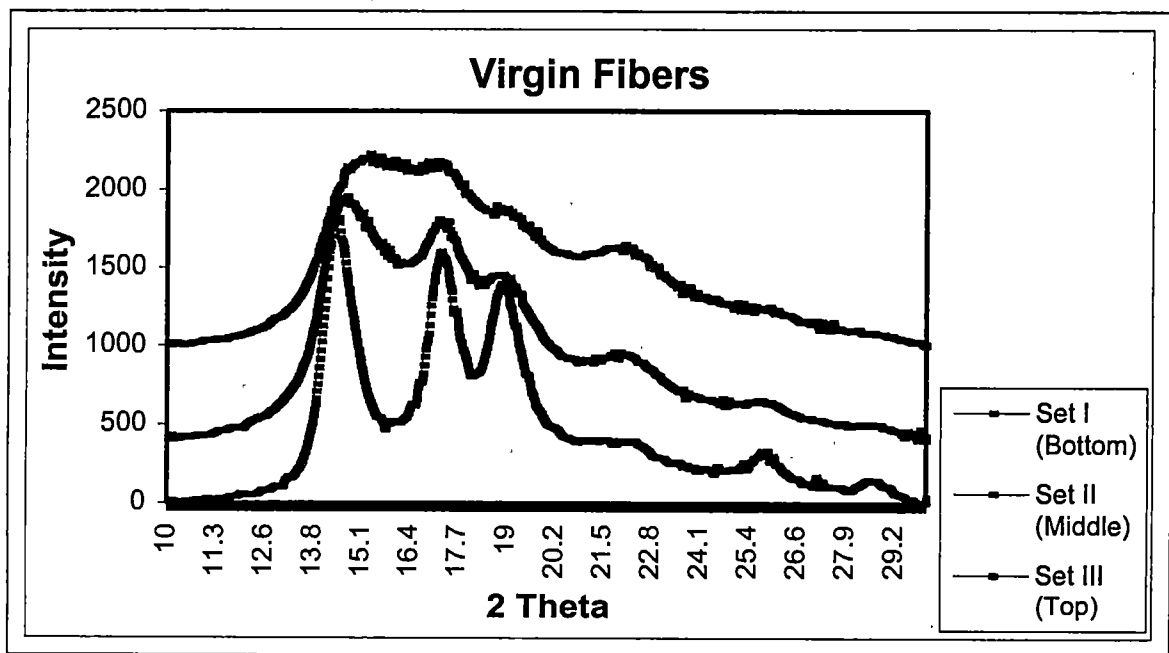
Figure 4.31 WAXD Equatorial Scans of Virgin Spunbond Fibers
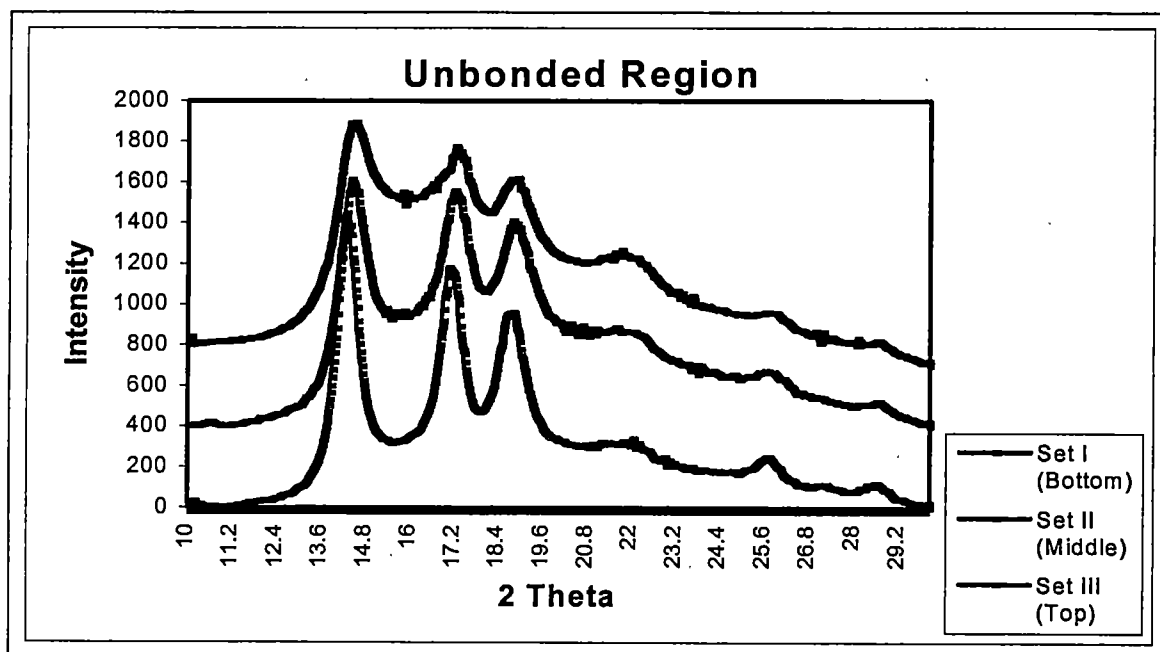
Figure 4.32 WAXD Equatorial Scans of Unbonded Regions (Spunbond)
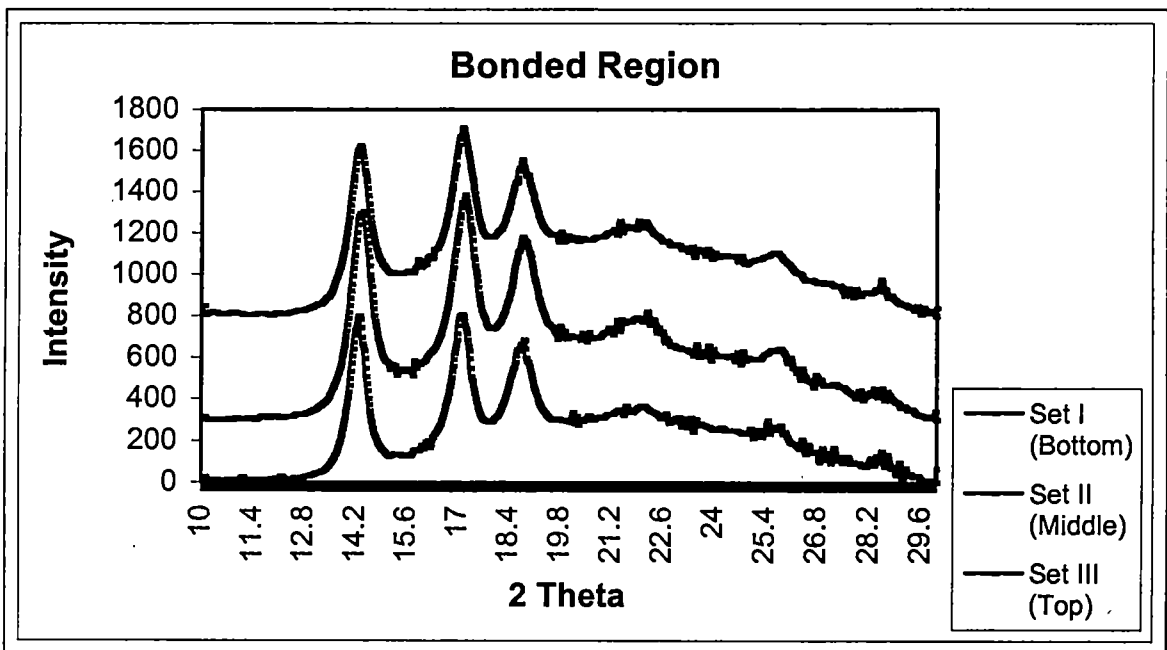
Figure 4.33 WAXD Equatorial Scans of Bonded Regions (Spunbond)

CHAPTER V

CONCLUSIONS

Fiber morphology plays a very important role in determining the optimum bonding conditions and the mechanical properties of the web. Fibers with relatively less developed morphology yielded stronger and tougher webs as compared to fibers with more developed morphology. The fibers with high molecular orientation and crystallinity tended to form a weak and brittle bond mainly due to lack of polymer flow and fibrillation of the fibers in bonded regions. Fiber breaking extension was found to be equally important, if not more, as fiber strength in governing the web properties. Higher breaking extension of the fibers leads to a greater degree of load sharing between the fibers during deformation, thus, improving the mechanical properties of the web. These observations were supported by failure analyses by SEM and single bond tensile tests. Fibers with less developed morphology showed lower optimum bonding temperature. A good correlation was observed between the bondability of the fibers and the thermomechanical stability of the fibers as measured by TMA. Drawn fibers having higher thermomechanical stability showed higher optimum bonding temperature as compared to as-spun fibers. It was also observed that optimizing the bonding temperature did not help much in improving the web properties in the case of highly drawn fibers, i.e., fibers with very high molecular orientation and crystallinity.

Spunbond studies also supported the above findings. In addition, it was observed that crystalline structure and crystal size do affect thermomechanical stability and, thus,

bondability of the fibers. Less perfect and less stable structure, such as smectic phase with smaller crystals in the case of Set III, led to lower thermomechanical stability and, thus, better bondability of the fibers. In general, bonding behavior of spunbond fibers was found to be similar to that of as-spun staple fibers.

It was observed that fibers do undergo significant structural changes in bonded as well as unbonded regions of the web during the thermal bonding process. The extent of change in fiber structure would depend upon the structure of original fibers and process variables employed. Structural changes included increase in birefringence, increase in crystallinity, increase in crystal size, transformation of smectic phase to more stable monoclinic phase. These structural changes in the fibers may be attributed to annealing and recrystallization of the fibers during thermal bonding.

REFERENCES

REFERENCES

1. Reed R., U.S. Patent 2277049, assigned to Kendall Company, 1942.

2. Dharmadhikary R. K., Gilmore T. F., Davis H. A., and Batra S. K. "Thermal Bonding of Nonwoven fabrics", *Textile Progress*, 26(1995), No. 2, pp. 1-37.

3. Bechter D., Roth A., Schaut G., Ceballos R., Kleinmann K., and Schafer K. "Thermal Bonding of Nonwovens", *Melliand Textilberichte*, 1997, No. 3, pp. E39-40.

4. Wei K. Y., Vigo T. L., and Goswami B. C. "Structure-Property Relationships of Thermally bonded Polypropylene Nonwovens", *J. Appl. Polym. Sci.*, 30(1985), No.4, pp. 1523-1534.

5. Wyatt N. E. and Goswami B. C. "Structure–Property Relationships in Thermally bonded Nonwoven Fabrics", *J. Coated Fabrics*, 14(1984), pp. 100-123.

6. Philipp P. "Thermal Bonding with Copolyester Melt Adhesive Fibers", *Nonwovens World*, Nov. 1986, pp. 81-85.

7. Riedel J. E. "Nonwovens Bonding Methods and Materials", *Nonwovens World*, May-June 1987, pp. 47-50.

8. Hoyle A. G. "Bonding as a Nonwoven Design Tool", *Tappi J.*, 1989, No.4, pp. 109-112.

9. Kwok W. K., Crane J. P., Gorrafa A., and Iyengar Y. "Polyester Staple fibers for Thermally Bonded Nonwovens", *Nonwovens Industry*, June 1988, pp. 30-33.

10. Warner S. B. "Thermal Bonding of Polypropylene Fibers", *Text. Res. J.*, 59(1989), pp. 151-159.

11. Wunderlich B. "Macromolecular Physics", Vol. 3, Academic Press, New York, NY, USA, 1980.

12. De Angelis V., DiGiaoacchino T., and Olivieri P. "Hot Calendered Polypropylene Nonwoven fabrics", Proceedings of 2nd International Conference on Polypropylene Fibers and Textiles, Plastics, and Rubber Institute, University of York, England, 1979, pp. 52.1-52.13.

13. Bechter D., Kurz G., Maag E., and Schutz J. "Thermal Bonding of Nonwovens", *Textil-Praxis*, 46(1991), pp. 1236-1240.

14. Malkan S. R., Wadsworth L. C., and Devis C. "Parametric Studies of the Reicofil Spunbonding Process", Third TANDEC Conference, 1993.

15. Malkan S. R., Wadsworth L. C., and Devis C. "Parametric studies of the Reicofil Spunbonding Process", *International Nonwovens Journal*, 1992, No.2, pp. 42-70.

16. Gibson P. E. and McGill R. L. "Thermally Bondable Polyester Fiber: the Effect of Calender Temperature", *Tappi J.*, 1987, No.12, pp. 82-86.

17. Beyreuther R. and Malcomess H. J. "Spunbonded Nonwovens-Linking Innovative Polymer, Technological and Textile Research", *Melliand Textilberichte*, 74(1993), No. 4, pp. E133-135.

18. Winchester S. C. and Whitwell J. C. "Studies of Nonwovens-I: A Multivariable Approach", *Text. Res. J.*, 40(1970), No.5, pp. 458-471.

19. Muller D. H. "How to Improve the Thermal Bonding of Heavy Webs", *INDA J. Nonwovens Res.*, 1989, No. 1, pp. 35-43.

20. Drelich A. "Thermal Bonding with Fusible Fibers", *Nonwovens Industry*, Sept.1985, pp. 12-26.

21. Philips P. J. and Tseng H. T. "Influence of Pressure on Crystallization in PET", *Macromolecules*, 22(1989), pp. 1649-1655.

22. Wishman M. and Gerald E. H., in "Handbook of Fiber Science and Technology" (Lewin M. and Pearce E. M., Ed.), Vol IV, New York, 1985, pp. 435-464.

23. Samuels R. J. "Structured Polymer Properties", Wiley, New York, 1974.

24. Samuels R. J., *Polym. Eng. Sci.*, 16(1976), p.327.

25. Ziabicki A. "Fundamentals of Fiber Formation", Wiley, New York, 1976.

26. Hagler G. E. "Qualitative Prediction of the Effects of Changes in Spinning Conditions on Spun Fiber Orientation", *Polym. Eng. Sci.*, 21(1981), pp. 121-123, Figs. 27, 46.

27. Sheehan W. C. and Cole T. B., *J. Appl. Polym. Sci.*, 8(1964), p. 2359.

28. Katayama K., Amano T., and Nakamura K., *Kolloid-Z Z. Polym.*, 1968, p. 125.

29. Fung P. Y. F., Orlando E., and Carr S. H. "Development of Stress-Crystallized Morphology During Melt Spinning of Polypropylene Fibers", *Polym. Eng. Sci.*, 13(1973), p. 295.

30. Kitao T., Ohya S., Furukawa S., and Yamashita S., "Orientation of Polymer Molecules During Melt Spinning-II: Orientation of Crystals in As-Spun Polyolefin Fibers", *J. Polym. Sci. Polym. Phys.*, 11(1973), pp. 1091-1094, Fig. 44.

31. Anderson P. G. and Carr S. H., *J. Mater. Sci.*, 10(1975), p. 870.

32. Henson H. M. and Spruiell J. E., Paper presented at Division of Cellulose, Paper, and Textile Chemistry, American Chemical Society, Philadelphia, April 1975.

33. Ishizuka O. and Koyama K. "Extensional Deformation and Orientation of a Running Filament in Melt Spinning", *Sen-i Gakkaishi*, 32(1976), No. 2, pp. T49-54.

34. Nadella H. P., Henson H. M., Spruiell J. E., and White J. L., "Melt Spinning of Isotactic Polypropylene: Structure Development and Relationship to Mechanical Properties", *J. Appl. Polym. Sci.*, 21(1977), No. 11, pp. 3003-3022.

35. Shimizu J., Tiriumi K., and Imai Y., *Sen-i Gakkaishi*, 33(1977), p. T-255.

36. Clark E. S. and Spruiell J. E., *Polym. Eng. Sci.*, 16(1976), p. 176.

37. Minoshima W., White J. L., and Spruiell J. E. "Experimental Investigations of the Influence of Molecular Weight Distribution on Melt Spinning and Extrudate Swell Characteristics of Polypropylene", *J. Appl. Polym. Sci.*, 25(1980), No. 2, pp. 287-306.

38. Petrelin A., *J. Mater. Sci.*, 6(1971), p. 490.

39. Peterlin A., *J. Polym. Sci.*, 17(1977), p. 183.

40. Petrelin A., in "Polymeric Materials", American Society for Metals, Metals Park, Ohio, 44073(1975).

41. Nadella H. P., Spruiell J. E., and White J. L. "Drawing and Annealing of Polypropylene Fibers: Structural and Mechanical Properties", *J. Appl. Polym. Sci.*, 22(1978), No. 11, pp. 3121-3133.

42. Kitao T., Spruiell J. E., and White J. L. "Influence of Drawing, Twisting, Heat Setting, and Up-twisting on the Structure and Mechanical Properties of Melt Spun Polypropylene Filament", *Polym. Eng. Sci.*, 19(1979), No. 11, pp. 761-773.

43. Sakthivel A., M. S. Thesis, Georgia Institute of Technology, 1983.

44. Balta-Calleja F. J. and Peterlin A., "Plastic Deformation of Polypropylene-V: Annealing of Drawn Polypropylene Fibers", *Macromol. Chem.*, 141(1971), Feb., pp. 91-116.

45. Jaffe M., in "Thermal Methods in Polymer Analysis" (Shalaby S. W., Ed.), Franklin Institute Press, Philadelphia, 1977, p. 93.

46. Samuels R. J. "Quantitative Structural Characterization of the Melting Behavior of Isotactic Polypropylene", *J. Polym. Sci., Polym. Phys.*, 13(1975), No. 7, pp. 1417-1446.

47. Katayama K., Amano T., and Nakamura K., *Kolloid Z. Z. Polymere*, 1968, p. 125.

48. Zhang D. "Fundamental Investigation of the Spunbonding Process", Ph.D. Thesis, The University of Tennessee @ Knoxville, 1995.

49. Backer S. and Petterson D. R. "Some Principles of Nonwoven Fabrics", *Text. Res. J.*, 30(1960), pp. 704-711.

50. Hearle J. W. S. and Stevenson P. J. "Studies in Nonwoven Fabrics-Part IV: Prediction of Tensile Properties", *Text. Res. J.*, 34(1964), pp. 181-191.

51. Hearle J. W. S. and Newton A. "Nonwoven Fabric studies-Part XV: The Application of Fiber Network Theory", *Text. Res. J.*, 38(1968), pp. 343-351.

52. Dent R. W., "The Initial Modulus of Filament Webs", Trans ASME, *J. Engi. Ind.*, 102(1980), pp. 360-365.

53. Hartman L., *TM*, 101(1974), No. 9, pp. 26-30.

54. Spruiell J. E., Misra S., and Richeson G. C. "Investigation of Spunbonding Process via Mathematical Modeling", *INDA Journal of Nonwovens Research*, 5(1993), No. 2, p. 13.

55. Storer R. A., ASTM, Easton, MD, USA, 1986.

56. Instructions Manual, Mettler Thermal Analysis System, p. 91.

57. Cullity B. D., "Elements of X-ray Diffraction", Addison-Wesley Publishing Company Inc., Massachusetts, 1978, p. 284.

58. INDA Standard Test, 1980.

59. Jr. Taylor W. N. and Clark E. S., *Polym. Eng. Sci.*, 18(1978), p. 518.

60. Hearle J. W. S. and Greer R., *Textile Progress*, 2(1970), No. 4 p. 162.

61. Ahmed M., "Polypropylene Fibers, Science and Technology", Elsevier Science Publishing Company, New York, 1982, p. 194

APPENDICES

APPENDIX I

SAS Output for 'Analysis of Variances' between Tenacity of Different Spunbond Fibers

The ANOVA Procedure

Dependent Variable: Ten_gpd_   Ten_gpd_

Source	DF	Sum of Squares	Mean Square	F Value	Pr > F
Model	2	2.26583021	1.13291511	11.33	0.0003
Error	27	2.70087456	0.10003239		
Corrected Total	29	4.96670477			

R-Square	Coeff Var	Root MSE	Ten_gpd_ Mean
0.456204	11.63262	0.316279	2.718897

Source	DF	Anova SS	Mean Square	F Value	Pr > F
Fibers	2	2.26583021	1.13291511	11.33	0.0003

APPENDIX II

SAS Output for 'Analysis of Variances' between Strength of Different Sets of Spunbond Webs at Different Bonding Temperatures

The ANOVA Procedure

------------------------------------- BondTemp=A (122 °C) -------------------------------------

Dependent Variable: Ten

Source	DF	Sum of Squares	Mean Square	F Value	Pr > F
Model	1	0.97957305	0.97957305	1.55	0.2222
Error	30	18.90790251	0.63026342		
Corrected Total	31	19.88747556			

R-Square	Coeff Var	Root MSE	Ten Mean
0.049256	34.88627	0.793891	2.275656

Source	DF	Anova SS	Mean Square	F Value	Pr > F
fiber	1	0.97957305	0.97957305	1.55	0.2222

------------------------------------- BondTemp=B (129 °C)-------------------------------------

Dependent Variable: Ten

Source	DF	Sum of Squares	Mean Square	F Value	Pr > F
Model	2	1.90894549	0.95447275	1.46	0.2433
Error	45	29.43947358	0.65421052		
Corrected Total	47	31.34841907			

R-Square	Coeff Var	Root MSE	Ten Mean
0.060894	23.50669	0.808833	3.440862

Source	DF	Anova SS	Mean Square	F Value	Pr > F
fiber	2	1.90894549	0.95447275	1.46	0.2433

------------------------------------- BondTemp=C (135 °C) -------------------------------------

Dependent Variable: Ten

Source	DF	Sum of Squares	Mean Square	F Value	Pr > F
Model	2	1.62646365	0.81323183	1.03	0.3666
Error	45	35.65781284	0.79239584		
Corrected Total	47	37.28427649			

R-Square	Coeff Var	Root MSE	Ten Mean
0.043623	22.75717	0.890166	3.911585

Source	DF	Anova SS	Mean Square	F Value	Pr > F
fiber	2	1.62646365	0.81323183	1.03	0.3666

------------------------------------- BondTemp=D (142 °C)-------------------------------------

Dependent Variable: Ten

Source	DF	Sum of Squares	Mean Square	F Value	Pr > F
Model	2	5.03115082	2.51557541	3.49	0.0391
Error	45	32.46721658	0.72149370		
Corrected Total	47	37.49836740			

	R-Square	Coeff Var	Root MSE	Ten Mean
	0.134170	25.49862	0.849408	3.331191

Source	DF	Anova SS	Mean Square	F Value	Pr > F
fiber	2	5.03115082	2.51557541	3.49	0.0391

------------------------------------- BondTemp=E (148 °C) -------------------------------------

Dependent Variable: Ten

Source	DF	Sum of Squares	Mean Square	F Value	Pr > F
Model	0	0.00000000	.	.	.
Error	15	11.11036702	0.74069113		
Corrected Total	15	11.11036702			

	R-Square	Coeff Var	Root MSE	Ten Mean
	0.000000	35.14447	0.860634	2.448847

Source	DF	Anova SS	Mean Square	F Value	Pr > F
fiber	0	0	.	.	.

APPENDIX III

SAS Output for 'Analysis of Variances' to See Significance of the Effect of Bonding Temperature on Spunbond Web Strength

The ANOVA Procedure

-- fiber=Set I --

Dependent Variable: Ten

Source	DF	Sum of Squares	Mean Square	F Value	Pr > F
Model	3	23.56554742	7.85518247	10.73	<.0001
Error	60	43.92683018	0.73211384		
Corrected Total	63	67.49237760			

R-Square	Coeff Var	Root MSE	Ten Mean
0.349159	25.57033	0.855637	3.346208

Source	DF	Anova SS	Mean Square	F Value	Pr > F
BondTemp	3	23.56554742	7.85518247	10.73	<.0001

-- fiber=Set II --

Dependent Variable: Ten

Source	DF	Sum of Squares	Mean Square	F Value	Pr > F
Model	3	33.11213880	11.03737960	15.35	<.0001
Error	60	43.13483581	0.71891393		
Corrected Total	63	76.24697461			

	R-Square	Coeff Var	Root MSE	Ten Mean
	0.434275	26.01510	0.847888	3.259215

Source	DF	Anova SS	Mean Square	F Value	Pr > F
BondTemp	3	33.11213880	11.03737960	15.35	<.0001

-- fiber=Set III --

Dependent Variable: Ten

Source	DF	Sum of Squares	Mean Square	F Value	Pr > F
Model	3	15.44420083	5.14806694	7.62	0.0002
Error	60	40.52110654	0.67535178		
Corrected Total	63	55.96530737			

	R-Square	Coeff Var	Root MSE	Ten Mean
	0.275960	26.02813	0.821798	3.157346

Source	DF	Anova SS	Mean Square	F Value	Pr > F
BondTemp	3	15.44420083	5.14806694	7.62	0.0002

VITA

Subhash Chand was born in Ghaziabad, India, on June 22, 1973. He did his schooling in his small village Chandner. He joined Indian Institute of Technology, Delhi (India) in August 1991 and received his Bachelor of Technology Degree in Textile Technology in May 1995. He worked in Vardhman Spinning & General Mills, Ltd., Ludhiana (India), as R&D Engineer from 1995 to 1997. In Spring 1998, he joined the Master's program in Textile Science at the University of Tennessee, Knoxville, where he received his degree in December 1999. He was employed as Graduate Research Assistant in the department of Textile Science during his stay at the University of Tennessee. His research interests are in polymer and fiber engineering.